



The Chemist

Journal of the American Institute of Chemists



In this Issue

- * *Phase Equilibria in the Tl_2Te - Tl_5Te_3 - Tl_9SmTe_6 System*
- * *Phytoremediation of Silver Species by Waterweed*
- * *Antifungal Activity of Silver Loaded Zeolite A from Bagasse Ash Against *Candida Albicans**
- * *3-Bromopyruvate and Genistein Combination Inhibits Glycolysis and Induces Cell Death in DU-145 and LNCaP Prostate Cancer Cells*
- * *Oxa-Bridged Donor-Acceptor Systems Containing Triazine Core for Dye Sensitized Solar Cell Applications*
- * *The Need for Nanometry Education*

Note: Dye-sensitized solar cell on the SwissTech Convention Center.
This work has been released into the public domain by author Giuseppe Peretto.
The file was taken from Wikimedia Commons from the following location:
https://commons.wikimedia.org/wiki/File:SwissTech_Convention_Center_-_Gr%C3%A4tzel.jpg

The Chemist

Established in 1923, The Chemist is the official publication of The American Institute of Chemists, Inc. (AIC). The Chemist was published quarterly in magazine format until 2006. The Chemist is currently being set up and formatted as an online journal.

Editor-in-Chief

David Devraj Kumar
Florida Atlantic University, USA

Editorial Assistants

Chelsea Dittrich
Florida Atlantic University, USA

Deborah Cate
The American Institute of Chemists, USA

Art & Web Direction

Alberto Fernández
Florida Atlantic University, USA

Editorial Review Board

John E. E. Baglin,..... *IBM Almaden Research Center, USA*
Rodney Bennett,..... *JRF America, USA*
Bethany Davis,..... *Clinlogix, LLC, USA*
Jerry Ray Dias,..... *University of Missouri-Kansas City, USA*
J. Stephen Duerr,..... *Chemlabconsulting, LLC, USA*
Lawrence Duffy,..... *University of Alaska Fairbanks, USA*
Peter D. Frade,..... *Wayne State University, USA*
Abraham George,..... *Mar Ivanios College, India*
David Gossman,..... *Gossman Consulting, Inc., USA*
Margaret Hall,..... *University of Southern Mississippi, USA*
Karickal. R. Haridas,..... *Kannur University, India*
John Hill,..... *La Trobe University, Australia*
Todd A. Houston,..... *Griffith University, Australia*
Esosa Iriowen,..... *Delaware State University, USA*
Jerry P. Jasinski,..... *Keene State College, USA*
Edward J. Kikta, Jr.,..... *FMC Corporation, USA*
David Devraj Kumar,..... *Florida Atlantic University, USA*
Gopendra Kumar,..... *University of Botswana, Botswana*
James Kumi-Diaka,..... *Florida Atlantic University, USA*
Gary R. List,..... *US Department of Agriculture, USA*
Bushan Mandava,..... *Mandava Associate, LLC, USA*
David M. Manuta,..... *Manuta Chemical Consulting, Inc., USA*
Dayal T. Meshri,..... *Advance Research Chemicals, Inc., USA*
E. Gerald Meyer,..... *University of Wyoming, USA*
Robert F. Moran,..... *Wentworth Institute of Technology, USA*
Wayne A. Morris,..... *Morris-Kopec Forensics, Inc., USA*
Ronald Persin,..... *Lnk2Lrn, USA*
Gary F. Porter,..... *Bergan Community College, USA*
Manit Rappon,..... *Lakehead University, Canada*
Sarah Reiser,..... *The Chemical Heritage Foundation, USA*
Henry F. Schaefer, III,..... *University of Georgia, USA*
James S. Smith,..... *Trillium, Inc., USA*
Joy E. Stewart,..... *Broward College, USA*
Saligrama Subbarao,..... *Lincoln University, USA*
P. V. Thomas,..... *Mar Ivanios College, India*
Ranjit K. Verma,..... *Magaah University, India*
Rock J. Vitale,..... *Environmental Standards, Inc., USA*
Kurt Winkelman,..... *Florida Tech, USA*

The American Institute of Chemists, Inc. does not necessarily endorse any of the facts or opinions expressed in the articles, book reviews, or advertisements appearing in The Chemist.

Subscription: \$35 per year to members, \$100 per year to non-members. Single copy: \$50.

The Chemist (ISSN-0009-3025) is published online by The American Institute of Chemists, Inc.

The Chemist

Journal of the American Institute of Chemists

Editorial: Augmenting the Scientific Mindset

David Devraj Kumar..... iii

ARTICLES

Phase Equilibria in the Tl_2Te - Tl_5Te_3 - Tl_9SmTe_6 System

S. Z. Imamaliyeva, V. A. Gasymov, M. B. Babanly..... 1

Phytoremediation of Silver Species by Waterweed

L. Bernas, K. Winkelman, A. Palmer 7

Antifungal Activity of Silver Loaded Zeolite A from Bagasse Ash
Against *Candida Albicans*

A. A. Widati, A. Baktir, R. Rachmawan 14

3-Bromopyruvate and Genistein Combination Inhibits Glycolysis and
Induces Cell Death in DU-145 and LNCaP Prostate Cancer Cells

H. Goldsmith, G. Kazdailyte, J. Kumi-Diaka 20

Oxa-Bridged Donor-Acceptor Systems Containing Triazine Core for
Dye Sensitized Solar Cell Applications

S. C. Subramanian, M. M. Velayudhan, M. Narayanapillai..... 23

The Need for Nanometry Education

D. D. Kumar 32

PUBLIC UNDERSTANDING OF CHEMISTRY

Building Interdisciplinary Bridges for Science

J. Baglin..... 34

The AIC Code of Ethics..... 38

Manuscript Style Guide 40

ANNOUNCEMENTS

Invitation to Authors 45



Editorial

Augmenting the Scientific Mindset

David Devraj Kumar

Florida Atlantic University

Scientists generally tend to view the natural world in terms of science. However, Isaac Newton, Robert Boyle, and Francis Bacon took this limited perspective off themselves and contributed to far-ranging and remote fields such as philosophy, arts, humanities, and theology. It is important that the scientific mindset be augmented so that science can continue to be a contributing member of the world in which we live. For example, chemical scientists working with artists and children's advocates have produced paints that are lead-free and child-friendly. As chemistry is an interconnecting and complementing field in the world of sciences, so are education, arts, social sciences, and humanities. Not only chemistry, but science in general needs more interdisciplinary "bridges" to other fields (1).

This issue of *The Chemist* has a lineup of thought-provoking and highly informative articles. S. Z. Imamaliyeva and co-authors reported an experimental study of phase equilibriums in the $Tl_2Te-Tl_5Te_3-Tl_9SmTe_6$ system. L. Bernas and co-authors investigated waterweed *Egeria Densa* as a proper candidate for photoremediation in aquatic environments. The study presented by A. A. Widati and co-authors demonstrated the preparation of silver loaded zeolite A from bagasse ash and its antifungal function against *Candida albicans*. A research communication by H. Goldsmith and co-authors addressed the effect of 3-Bromopyruvate and Genistein combination on prostate cancer cells. S. C. Subramanian and co-authors explored the use of oxa-bridged donor-acceptor systems with Triazine core in dye sensitized solar cell applications. D. D. Kumar addressed the need for nanometry education. In the Public Understanding of Chemistry Section, J. E. E. Baglin argued in favor of interdisciplinary bridges in science.

The Chemist Volume 90, Issue Number One presents a reorganized Editorial Review Board. I appreciate all the hard work of the members of the Review Board who reviewed manuscripts in a timely manner and contributed to improve the quality of the Journal.

References

J. E. E. Baglin, *The Chemist*, 90 (2017)

Phase Equilibria in the Tl_2Te - Tl_5Te_3 - Tl_9SmTe_6 System

Samira Zakir Imamaliyeva*, Vagif Akber Gasymov, Mahammad Baba Babanly

Institute of Catalysis and Inorganic Chemistry named after acad. M. Nagiyev

National Academy of Science of Azerbaijan, H. Javid Ave., 131, Az-1143, Baku, Azerbaijan

(*E-mail: samira9597a@gmail.com)

Abstract: Phase equilibria in the Tl_2Te - Tl_5Te_3 - Tl_9SmTe_6 system were experimentally studied by means of differential thermal analysis, powder X-ray diffraction technique and microhardness measurements applied to equilibrated alloys. Several isopleth sections and isothermal section at 300 K, as well as projections of the liquidus and solidus surfaces, were constructed based on the experimental data. It was established that homogeneity area of solid solutions with Tl_5Te_3 structure (δ -phase) occupied more than 90% of the concentration triangle. A narrow area of solid solutions (α -phase) based on Tl_2Te was detected.

Key Words: thallium-samarium tellurides, phase equilibria, solid solutions, crystal structure.

INTRODUCTION

Chalcogenides of heavy p-elements have received a lot of attention thanks to their interesting functional properties, such as thermoelectric, photoelectric, optical, magnetic properties [1-3]. Furthermore, in recent years some of such compounds have attracted both scientific and technological interest as topological insulators [4-6]. Doping by rare-earth elements can improve their properties and give them additional functionality, such as the magnetic properties [7,8].

Thallium subtelluride, Tl_5Te_3 is suitable "matrix" for creation of new complex materials. This compound crystallizes in tetragonal structure [9] (Sp.gr. I4/mcm) with four formula units per unit cell (Fig.1). The basic structural component of Tl_5Te_3 compound is octahedron with a thallium atom, Tl(2), in its center. These octahedra connected by vertices form a frame Tl_4Te_{12} , or $(TlTe_3)_4$. The other 16 thallium atoms, Tl(1) link octahedra along the c axis and form a unit cell $Tl_{16}(TlTe_3)_4$. B^{3+} (B^{3+} -Sb, Bi) substitution for half of the Tl(2) atoms, resulting in the

compounds Tl_9BTe_6 or $Tl_{16}[(Tl_{0.5}^{1+}B_{0.5}^{3+})Te_3]_4$ (I), while the replacement of all these thallium atoms by cations A^{2+} (A^{2+} -Sn, Pb) leading to formation of Tl_4ATe_3 or $Tl_{16}[A^{2+}Te_3]_4$ (II).

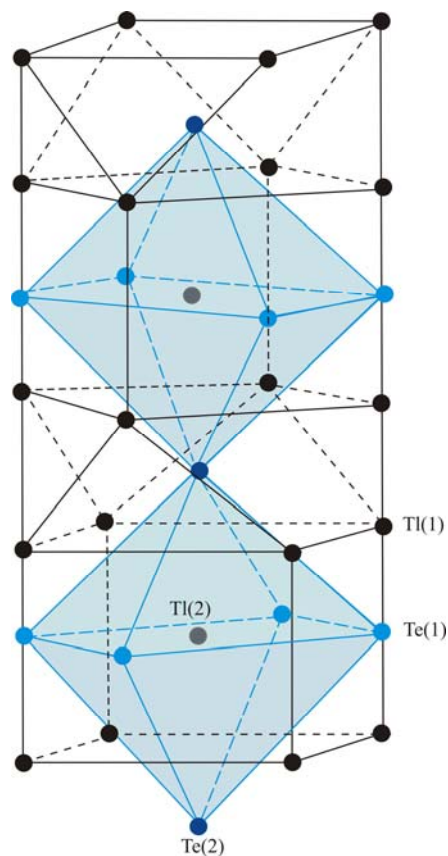


Fig 1. Basic structural component of Tl_5Te_3 compound.

Compounds of type (I) and (II) were detected during the experimental phase equilibria studies of respective ternary systems [10-13]. These materials possess thermoelectric properties, and Tl_9BiTe_6 was found to have the highest ZT value [1,2,14].

A new thallium lanthanide tellurides with composition Tl_9LnTe_6 (Ln-Ce, Nd, Sm, Gd, Tm, Tb) were obtained first by Babanly M.B. [15-17]. It was shown that above mentioned compounds are substitution variants of Tl_5Te_3 , and their melting character and crystal lattices parameters were determined. Moreover, ytterbium does not form the compound Tl_9YbTe_6 [17, 18]. Later, the crystal structure as well as magnetic and thermoelectric properties for a number Tl_9LnTe_6 -type compounds were determined by authors [19-21].

According to the phase diagrams [10-13, 15], all listed ternary compounds are phases with variable composition and have wide homogeneity areas.

In our previous papers [22-25], we have presented the results of phase equilibria investigations of the Tl_5Te_3 - Tl_9NdTe_6 - Tl_9BiTe_6 , Tl_5Te_3 - Tl_4PbTe_3 - Tl_9NdTe_6 , Tl_9NdTe_6 - Tl_9BiTe_6 - Tl_4PbTe_3 , Tl_2Te - Tl_9NdTe_6 - Tl_9BiTe_6 , and Tl_2Te - Tl_9TbTe_6 systems including Tl_5Te_3 compound or its structural analogues. We found that the former three systems are characterized by formation of continuous solid solutions and the latter two systems- by wide areas of solid solutions.

Here we represent a detailed investigation of phase relationships of the Tl-Sm-Te system in the Tl_2Te - Tl_5Te_3 - Tl_9SmTe_6 composition area.

Tl_2Te and Tl_5Te_3 compounds melt congruently at 698 and 723 K and form the eutectic (695 K, ~ 34 at.% Tl) [26]. These data were confirmed by Okamoto [27]. Tl_2Te crystallizes in the monoclinic system (space group $C2/c$; $a = 15.662$; $b = 8.987$; $c = 31.196$ Å, $\beta = 100.76^\circ$, $z = 44$) [28], while tetragonal lattice parameters of Tl_5Te_3 are equal to $a = 8.930$; $c = 12.598$ Å [9]. Tl_9SmTe_6 melts with decomposition by the peritectic reaction at 755 K and has lattice constant: $a = 8.888$; $c = 13.013$ Å, $z = 2$ [16].

EXPERIMENTAL

Materials and Syntheses

Starting compounds Tl_2Te and Tl_5Te_3 were synthesized by melting of high purity elements in evacuated ($\sim 10^{-2}$ Pa) quartz ampoules at 750 K with following slow cooling. Tl_9SmTe_6 was synthesized at 1000 K using the ceramic method. Taking into account the

incongruent melting of Tl_9SmTe_6 [16], this compound was annealed at 700 K for 300 h after the synthesis.

The purity of the synthesized compounds was checked by differential thermal analysis (DTA) and powder X-ray diffraction (XRD) techniques.

Alloys of the Tl_2Te - Tl_5Te_3 - Tl_9SmTe_6 system were prepared by melting the stoichiometric quantities of the pre-synthesized binary and ternary compounds in evacuated silica ampoules at 900 K in a tube furnace. After the synthesis, alloys were powdered in an agate mortar, pressed into pellets and reheated at 680 K within 1000 h. In order to prevent a reaction between the ampoules and samarium, the silica tubes were coated with a carbon film via the decomposition of ethanol.

Methods

DTA and XRD analyses as well as microhardness measurements were employed to analyze the samples.

DTA was performed using a NETZSCH 404 F1 Pegasus differential scanning calorimeter. The crystal structure was analyzed by a powder X-ray diffraction technique at room temperature using a Bruker D8 diffractometer utilizing $\text{CuK}\alpha$ radiation within $2\theta = 10$ to 70° . Microhardness measurements were done with a microhardness tester PMT-3, the typical loading being 20g.

RESULTS & DISCUSSION

The combined analysis of experimental data enabled us to construct the self-consistent diagram of the phase equilibria in the Tl_2Te - Tl_5Te_3 - Tl_9SmTe_6 system (Table, Fig.2-7).

The (16/3) Tl_2Te - Tl_9SmTe_6 system (Fig.2) is a part of the Tl_2Te - Sm_2Te_3 system. It is a non-quasi-binary because of the incongruent character of the Tl_9SmTe_6 melting. However, it behaves as a quasi-binary system below the peritectic horizontal at 755 K. The phase diagram is characterized by formation of a wide area of solid solutions (δ) with the Tl_5Te_3 structure. Liquidus consists of three curves corresponding to the primary crystallization of α - and δ - phases based on Tl_2Te and Tl_9SmTe_6 , as well as the unknown infusible X phase (presumably TlSmTe_2). Horizontals at 755 and 703 K correspond to peritectic equilibria $L+X \leftrightarrow \delta$ and $L+\delta \leftrightarrow \alpha$. The peritectic points p_1 and p_2 correspond to 65 and 5 mol% Tl_9SmTe_6 , respectively.

The equilibrium phase diagram of the $2\text{Tl}_5\text{Te}_3$ - Tl_9SmTe_6 system (Fig.3) is also non-quasi-binary due to

peritectic melting of Tl_9SmTe_6 compound. This system is characterized by the formation of a continuous series of solid solutions (δ) based on Tl_5Te_3 . The δ -solid solutions primarily crystallize in 0-65 mol% Tl_9SmTe_6 composition area; whereas in region more than 65 mol% Tl_9SmTe_6 , the

X phase crystallizes. In this composition area below 755 K, a three-phase area $L+X+\delta$ should be formed as the result of monovariant peritectic reaction $L+X\leftrightarrow\delta$. However, this area is not experimentally fixed due to narrow temperature interval and shown by dashed line (Fig.3a).

Table 1. Some properties of phases in the $\text{Tl}_2\text{Te}-\text{Tl}_5\text{Te}_3-\text{Tl}_9\text{SmTe}_6$ system.

System	Phase	Thermal effects, K	Sp.gr	Lattice parameters, Å	H_μ , MPa
	Tl_2Te	698	monoclinic, $C2/c$;	$a = 15.662$; $b = 8.987$; $c = 31.196$ Å, $\beta = 100.760$, $z = 44$	1400
	Tl_5Te_3	723	tetragonal, $I4/mcm$	$a=8.930$; $c=12.598$	1130
	Tl_9SmTe_6	755; 1180	"-"	$a=8.888$; $c=13.013$	1080
$2\text{Tl}_5\text{Te}_3-$ Tl_9SmTe_6	$\text{Tl}_{9,8}\text{Sm}_{0,2}\text{Te}_6$	725-733	"-"	$a=8.922$; $c=12.681$	1130
	$\text{Tl}_{9,6}\text{Sm}_{0,4}\text{Te}_6$	730-740	"-"	$a=8.913$; $c=12.764$	1170
	$\text{Tl}_{9,5}\text{Sm}_{0,5}\text{Te}_6$	735-743	-		
	$\text{Tl}_{9,4}\text{Sm}_{0,6}\text{Te}_6$	735-745	"-"	$a=8.905$; $c=12.847$	1150
	$\text{Tl}_{9,2}\text{Sm}_{0,8}\text{Te}_6$	742-750; 1110	"-"	$a=8.896$; $c=12.930$	1120
$\frac{16}{3}\text{Tl}_2\text{Te}-$ Tl_9SmTe_6	$\text{Tl}_{9,8}\text{Sm}_{0,2}\text{Te}_{5,2}$	703-728	"-"	-	1240; 1480
	$\text{Tl}_{9,6}\text{Sm}_{0,4}\text{Te}_{5,4}$	713-747	"-"	$a=8.912$; $c=12.782$	1200
	$\text{Tl}_{9,6}\text{Sm}_{0,5}\text{Te}_{5,5}$	723-752	-		
	$\text{Tl}_{9,4}\text{Sm}_{0,6}\text{Te}_{5,6}$	733-755	"-"	$a=8.903$; $c=12.864$	1190
	$\text{Tl}_{9,2}\text{Sm}_{0,8}\text{Te}_{5,8}$	742-755; 1112	"-"	$a=8.894$; $c=12.955$	1150

The results of the microhardness measurements are in agreement with constructed phase diagram (Figs.2b and 3b). For the $\text{Tl}_5\text{Te}_3-\text{Tl}_9\text{SmTe}_6$ system, a curve has a flat maximum (Fig.3b), which is typical for systems with continuous solid solutions. For the $\text{Tl}_2\text{Te}-\text{Tl}_9\text{SmTe}_6$ system, the microhardness values of starting compounds are increased within homogeneity areas of α - and δ -phases, and remain constant in the $\alpha+\delta$ two-phase region (Fig.2b).

Powder X-ray analysis data confirm the phase diagrams of the above-mentioned systems (Fig.4). For the $\text{Tl}_5\text{Te}_3-\text{Tl}_9\text{SmTe}_6$ system, powder diffraction patterns of starting compounds and intermediate alloys are qualitatively similar with slight reflections displacement from one compound to another (Fig.4, diffraction patterns 4-6). For example, we present the powder diffraction pattern of alloy with 50 mol% Tl_9SmTe_6 . Solid solutions obey the Vegard's law, i.e. the lattice parameters depend linearly on composition. In the $\text{Tl}_2\text{Te}-\text{Tl}_9\text{SmTe}_6$ system, the alloys with compositions ≥ 30 mol% Tl_9SmTe_6 are monophasic with Tl_5Te_3 -type diffraction patterns (Fig.4, diffraction pattern 3), while alloy with 25mol% Tl_9SmTe_6

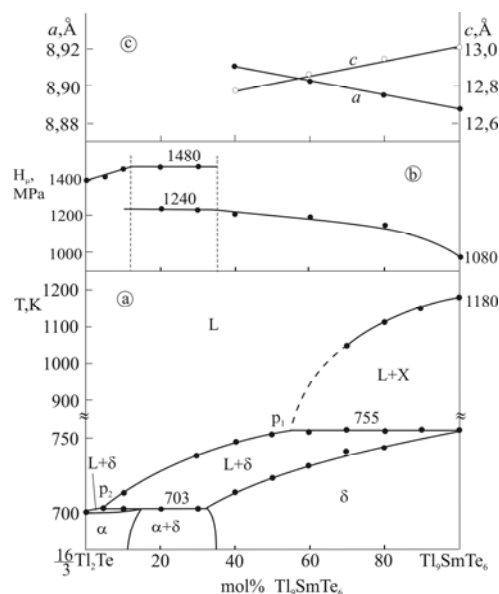


Fig 2. Phase diagram (a), concentration relations of microhardnesses (b), and lattice parameters (c) for the system $(16/3)\text{Tl}_2\text{Te}-\text{Tl}_9\text{SmTe}_6$.

composition is bi-phasic. Besides the δ -phase reflections this alloy contains weak peaks of α -phase (Fig.4, diffraction pattern 2).

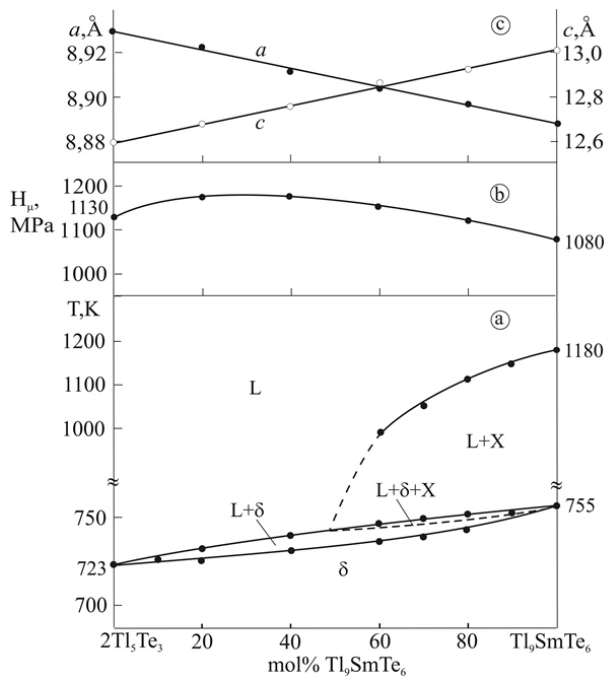


Fig 3. Phase diagram (a), concentration relations of microhardnesses (b), and lattice parameters (c) for the system $2\text{Ti}_5\text{Te}_3\text{-Tl}_9\text{SmTe}_6$.

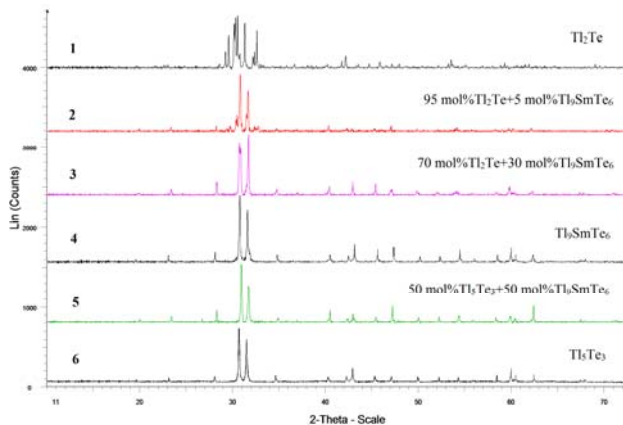


Fig 4. XRD patterns for different compositions in the $\text{Tl}_2\text{Te-Tl}_9\text{SmTe}_6$ (patterns 1-4) and $\text{Tl}_5\text{Te}_3\text{-Tl}_9\text{SmTe}_6$ (patterns 4-6) systems.

Isopleth sections of the $\text{Tl}_2\text{Te-Tl}_5\text{Te}_3\text{-Tl}_9\text{SmTe}_6$ system (Fig.5).

Figs. 5a-c show the isopleth sections $\text{Tl}_5\text{Te}_3\text{-[A]}$, $\text{Tl}_9\text{SmTe}_6\text{-[B]}$ and $\text{Tl}_2\text{Te-[C]}$ of the $\text{Tl}_2\text{Te-Tl}_5\text{Te}_3\text{-Tl}_9\text{SmTe}_6$ system, where A, B and C are alloys from the respective boundary system. As can be seen, over the entire compositions range of the $\text{Tl}_5\text{Te}_3\text{-[A]}$ system only δ -phase crystallizes from the melt.

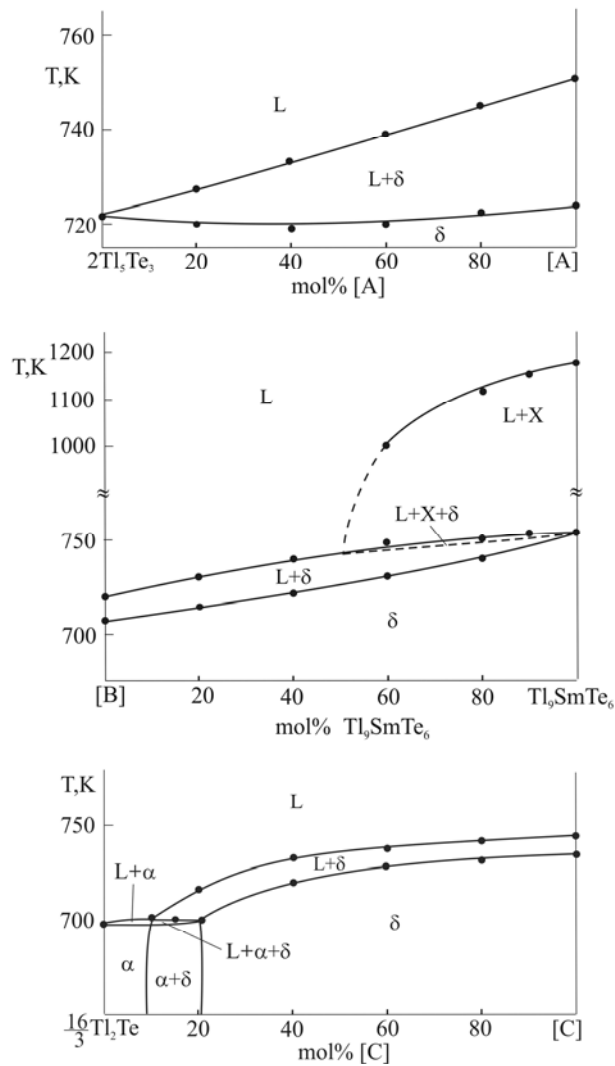


Fig 5. Polythermal sections $2\text{Ti}_5\text{Te}_3\text{-[A]}$, $\text{Tl}_9\text{SmTe}_6\text{-[B]}$ and $(16/3)\text{Tl}_2\text{Te-[C]}$ of the phase diagram of the $\text{Tl}_2\text{Te-Tl}_5\text{Te}_3\text{-Tl}_9\text{SmTe}_6$ system.

According to the phase diagram of the Tl_9SmTe_6 -[B] section in the composition area <50 mol% Tl_9SmTe_6 , the primary crystallization of the δ -phase occurs from the liquid phase. In the Tl_9SmTe_6 -rich alloys the X-phase first crystallizes, then a monovariant peritectic equilibrium $L+X\leftrightarrow\delta$ takes place.

The liquidus of Tl_2Te -[C] section consists of two curves of primary crystallization of α - and δ -phases. The intersection point of these curves corresponds to the monovariant peritectic reaction $L+\delta\leftrightarrow\alpha$ (703 K). Below the solidus, this section passes through the α , $\alpha+\delta$ and δ phase areas.

The isothermal sections of the Tl_2Te - Tl_5Te_3 - Tl_9SmTe_6 system at 300 K (Fig.6)

The isothermal sections of the Tl_2Te - Tl_5Te_3 - Tl_9SmTe_6 system at 300 K (Fig.6) consists of three phase areas. Over 90% of the concentration triangle is occupied by δ -solid solutions with Tl_5Te_3 structure. α -phase based on Tl_2Te has a narrow homogeneity area in the corresponding angle of the triangle. Homogeneity areas of the α - and δ -phases are separated by $\alpha+\delta$ two-phase region.

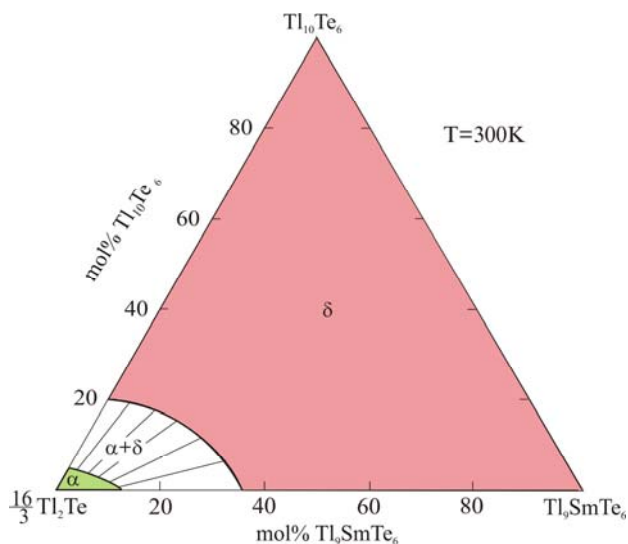


Fig 6. Isothermal section of the phase diagram of the Tl_2Te - Tl_5Te_3 - Tl_9SmTe_6 system at 300 K.

The liquidus surface projection (Fig.7)

Liquidus of Tl_2Te - Tl_5Te_3 - Tl_9SmTe_6 system consists of three fields of the primary crystallization of α -, δ - and

X-phases. These fields are separated by p_2e and p_1p_1' lines, which correspond to the monovariant peritectic equilibria $L+\delta\leftrightarrow\alpha$ and $L+X\leftrightarrow\delta$. Near the eutectic point (e) the peritectic equilibrium $L+\delta\leftrightarrow\alpha$ must be transformed into $L\leftrightarrow\alpha+\delta$ eutectic equilibrium. However, coordinates of this transformation are not experimentally fixed due to narrow temperature range. Solidus surface consists of two areas corresponding to the completion of crystallization α - and δ -phases.

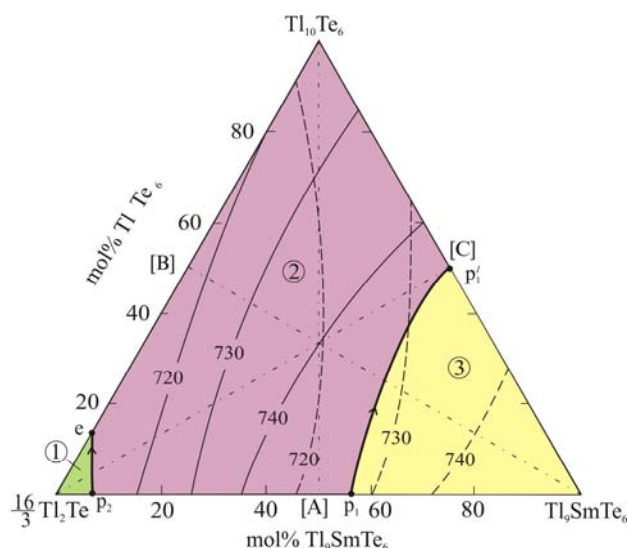


Fig 7. Projection of the liquidus and solidus (dashed lines) surfaces of the Tl_2Te - Tl_5Te_3 - Tl_9SmTe_6 system. Primary crystallization fields of phases: 1- α ; 2- δ ; 3-X. Dash-dot lines show the investigated sections.

CONCLUSION

A complete T-x-y diagram of the Tl_2Te - Tl_5Te_3 - Tl_9SmTe_6 system is constructed, including the T-x diagrams of boundary systems Tl_5Te_3 - Tl_9SmTe_6 and Tl_2Te - Tl_9SmTe_6 , some isopleth sections, isothermal section at 300 K and liquidus and solidus surface projections. Studied system is characterized by the formation of wide field of δ -solid solutions with the Tl_5Te_3 structure, occupying more than 90% of the concentration triangle. Obtained experimental data can be used for choosing the composition of solution-melt and for determining of temperature conditions for growing crystals of δ - phase with a given composition.

ACKNOWLEDGMENT

The work was supported by the Science Foundation of the State Oil Company of Azerbaijan Republic (Grant for the project "Preparation and investigation of new functional materials based on complex metal chalcogenides for alternative energy sources and electronic engineering", 2014).

REFERENCES

1. Shevelkov AV. *Russ. Chem. Rev.*, 2008, 77, 1.
2. *CRC Handbook of Thermoelectrics*, ed. by D. M. Rowe. CRC Press, New York, 1995, 701p.
3. Koc H, Simsek S, Mamedov AM & Ozbay E. *Ferroelectrics*, 2015, 483(1), 43.
4. Niesner D, Otto S, Hermann V, Fauster Th, Menshchikova TV, Ereemeev SV, Aliev ZS, Amiraslanov IR, Echenique PM, Babanly MB, Chulkov EV. *Phys.Rev.B*, 2014, 89, 081404.
5. Politano A, Caputo M, Nappini S, Bondino F, Aliev ZS, Babanly MB, Chulkov EV. *J.Phys.Chem.C*, 2014, 118, 21517.
6. Yan B, Zhang H-J, Liu C-X, Qi X-L, Frauenheim T and Zhang S-C. *Phys. Rev.B*, 2010, 82, 161108(R).
7. Alemi A, Klein A, Meyer G, Dolatyari M and Babalou AZ. *Anorg. Chem*, 2011, 637, 87.
8. Wu F, Song H, Jia J, Xu H. *Prog.Nat.Sci*, 2013, 23 (4), 408.
9. Schewe I, Böttcher P, Schnering HG. *Z.Kristallogr*, 1989, Bd188, 287.
10. Babanly MB, Akhmad'ar A, Kuliev AA. *Russ. J. Inorg. Chem*, 1985, 30, 1051.
11. Babanly MB, Akhmad'yar A, Kuliev AA. *Russ.J.Inorg. Chem*, 1985, 30, 2356.
12. Babanly MB, Gotuk A A, Kuliev AA. *Inorg.Mater*, 1979, 15, 1011.
13. Gotuk AA, Babanly M B, Kuliev AA. *Inorg. Mater*, 1979, 15, 1062.
14. Wolfing B, Kloc C, Teubner J, Bucher E. *Phys. Rev. Lett*, 2001, 36 (19), 4350.
15. Imamaliyeva SZ, Sadygov FM, Babanly MB. *Inorg.Mater*, 2008, 44, 935.
16. Babanly MB, Imamaliyeva SZ, Babanly DM. *Azerb.Chem.J*, 2009, 2, 121.
17. Babanly MB, Imamaliyeva SZ, Sadygov FM. *News of BSU. Nat. Sci.Ser*, 2009, 4, 5.
18. Imamaliyeva SZ, Mashadiyeva LF, Zlomanov VP, Babanly MB. *Inorg.Mater*, 2015, 51, 1237.
19. Bangarigadu-Sanasy S, Sankar C R, Assoud A, Kleinke H. *Dalton Trans*, 2011, 40, 86.
20. Bangarigadu-Sanasy S, Sankar C R, Schlender P, Kleinke H. *J. Alloys Compd*, 2013, 549, 126.
21. Bangarigadu-Sanasy S, Sankar CR, Dube PA, Greedan JE, Kleinke H. *J.Alloys. Compd*, 589, (2014) 389.
22. Babanly MB, Tedenac J-C., Imamaliyeva SZ, Guseynov FN, Dashdieva GB. *J.Alloys Compd*, 2010, 491, 230.
23. Imamaliyeva SZ, Guseynov FN, Babanly MB. *J. Chem. Probl*, 2008, 4, 640.
24. Imamaliyeva SZ, Guseynov FN, Babanly M. *Azerb.Chem.J*, 2009, 1, 49.
25. Imamaliyeva SZ, Gasanly TM, Sadygov FM, Babanly MB. *Azerb.Chem.J*, 2015, 3, 93.
26. Asadov MM, Babanly MB, Kuliev AA. *Inorg. Mater*, 1977, 13(8), 1407.
27. Okamoto H. *J. Phase Equilib*, 2001, 21(5), 501.
28. Cerny R, Joubert J, Filinchuk Y, Feutelais Y. *Acta Crystallogr. C*, 2002, 58(5), 163.

Phytoremediation of Silver Species by Waterweed

(*Egeria Densa*)

Leonard Bernas,^{1*} Kurt Winkelmann,¹ Andrew Palmer²

^{1*} Department of Chemistry, Florida Institute of Technology
150 West University Blvd, Melbourne, FL 32901

² Department of Biological Sciences, Florida Institute of Technology
150 West University Blvd, Melbourne, FL 32901

(*E-mail: lbernas2011@my.fit.edu)

Abstract: Silver species pose a threat to aquatic environments. *Egeria densa* (also known as *Elodea densa*), a common waterweed, was exposed to silver cations and humic acid-coated silver nanoparticles (AgNps) in an aqueous environment for 7 days. *E. densa* was chosen for this study because it is a fast-growing aquatic organism that also serves as a model for studies of heavy metal toxicity. Plants absorbed Ag⁺ and AgNps at concentrations as low as 5 ppm and significant effects on plant health were observed. Bioaccumulation of silver was positively correlated with the concentration of both Ag⁺ and AgNps. The substantial bioaccumulation of both silver species supports *E. densa* as a suitable candidate for phytoremediation in aquatic environments.

Key Words: *Egeria densa*, nanotechnology, phytoremediation, silver absorption, silver nanoparticles.

INTRODUCTION

Silver Nanoparticles

Nanotechnology is the study of chemical and physical interactions on the scale of 1-100 nm, a size range in which matter possesses distinct properties from both individual atoms and bulk particles. Nanomaterials are used for medicinal applications, environmental remediation, consumer products, and electronics. Silver nanoparticles (AgNps) in particular have been incorporated into 24% of almost 2000 consumer products containing nanoparticles [1]. They have diverse applications and are becoming more common in industrial processes. Small AgNps (<10 nm) can be more toxic to bacteria relative to Ag⁺ because of differences in size, shape, surface properties, and coating characteristics [2]. This enhanced toxicity has led to the increased use of AgNps as an antimicrobial agent. The increased fabrication and use of AgNps poses threats to aquatic ecosystems.

Although the U.S. Environmental Protection Agency (EPA) has regulated Ag⁺ release since 1980, the growing use of AgNps over the past 10 years requires that the environmental impacts of these particles be thoroughly examined to determine their long-term effects on our waterways and aquatic ecosystems. Sources of silver pollutants include waste from natural leaching, mining, and the photography industry. While silver salt discharges into the environment have decreased, silver toxicity remains a concern due to their increased use in consumable products. The fate of AgNps has been estimated based on models in aquatic systems, and indicate adverse effects depending on natural organic matter concentrations, ionic strength, and electrostatic effects between nanoparticle coatings and water composition [3]. For example, the oxidation of AgNps can also contribute to silver cation concentrations in water.

The presence of silver species in the environment, particularly the water supply, can result in bioaccumulation across multiple trophic levels with potentially toxic effects. While plants can be used for phytoremediation of silver species, the effects on fish and

other food sources can be devastating to the food chain. The EPA regulates total silver in aquatic environments, ensuring concentrations are 1.2-13 ppb (depending on CaCO_3 concentration) to limit the impacts on an ecosystem [4]. In addition, aquatic ecosystems are prone to silver contamination because of its increased uses manufacturing items such as soaps, textiles, and plastics [5]. While accidental discharges of silver compounds have declined after the 1970s, it is still estimated that 2500 tons of silver are released into waterways each year and that 80 tons ends up in surface waters [5, 6]. Silver nitrate is the most toxic form of silver because of its dissociation into Ag^+ . Other silver species have been identified as less toxic because they are largely insoluble, including complexes with chlorides and sulfides [6]. Increased understanding of nanoparticle behavior has led to greater focus on the effects of these particles on ecosystems.

Mechanisms of Silver Species Toxicity

Silver nanoparticles and Ag^+ have distinct mechanisms of toxicity but both are lethal to a variety of organisms, including bacteria, plants, animals, and fish in aquatic ecosystems [5, 7]. Silver species can damage the cellular structure and organelles through unfavorable binding interactions [8]. Further, size-based translocation of silver species is attributed to differences in toxicity between Ag^+ , insoluble silver salts, and AgNps [5, 6].

Silver cations enter the cell through transmembrane sodium and copper ion transporters and can accumulate in organisms [5]. These cations inhibit respiratory enzymes, induce oxidative stress, and bind to molecules containing sulfur and phosphorous [8]. Silver species exhibit a strong affinity for thiol groups on proteins and enzymes, causing the inactivation of these macromolecules due to formation of Ag-S bonds [9].

Two methods of translocation into the cell have been proposed. The first is by the association of the nanoparticle to the cell wall and release of Ag^+ [5]. Silver cations released by the AgNps cause damage through interference with the mitochondria, as seen in toxicity experiments with *Lemna gibba* (duckweed) [10]. Since AgNps can attach to the cell wall, any Ag^+ released due to the oxidation of the nanoparticles has a greater likelihood of entering the cell.

In the second mechanism for toxicity, AgNps enter the cell through endocytosis, caused by the invagination of the plasma membrane. Vesicles form and disperse

particles throughout the cell. Transmission electron microscopy (TEM) images of plant seedlings have demonstrated particle translocation in plants [11]. The association of AgNps with the active sites of proteins has been observed in the bacteria *Escherichia coli* and suggests that, depending on the coating, nanoparticle-protein association can decrease or inhibit enzyme and protein activity [12].

Phytoremediation of Heavy Metals

Phytoremediation is a green method used to remove contamination from terrestrial and aquatic environments based on the absorption and accumulation of heavy metals or toxins by plants [13]. Aquatic macrophytes are used for phytoremediation of toxic metals and *E. densa* effectively removes heavy metal cations from water. There are diverse applications of phytoremediation in aquatic plant systems, including re-harvesting toxins in plants unaffected by heavy metal uptake (phytoextraction) and absorption/adsorption of heavy metals by plant root systems (rhizofiltration). Both applications remove contaminants from the ecosystem.

Humic Acid Reduction of Ag^+ to Form AgNps

The reduction of AgNO_3 to AgNps in the presence of humic acids has been reported and is well characterized [14-16]. Humic acids are large polymers composed of organic structures found in soils and other geological features. Structures of humic acids vary by sampling location, but common characteristics include aromatics, heterocycles, carboxyls, and nitrogen content [17]. Humic acids used in these experiments are from the Suwannee River (GA), and the samples are generally consistent in the composition of the constituent functional groups and components [18]. Suwannee River humic acids have the following elemental composition: 52-53% C, 4-4.5% H, 42-43.5% O, 0.5-0.75% N, 0.4-0.6% S, and trace amounts of P.

Humic acid reduction of Ag^+ yields nanoparticles that remain stable for approximately 2 months, based on spectroscopic measurements [14]. This reduction indicates that AgNps may form under environmentally relevant conditions. Many acute toxicity studies of AgNps have been performed using methods that assume ideal accumulation, dispersion, and suspension [16]. While useful, these conditions are not environmentally relevant. *E. densa* is an aquatic macrophyte used in phytotoxicity

tests and pollution modeling due to its ability to accumulate contaminants and heavy metals. No studies have been conducted on the ability of the waterweed, *E. densa*, to absorb and remove silver species from an aqueous environment. This study investigated the absorption of Ag⁺ and AgNps by *E. densa* as part of a larger study of silver toxicity towards plants.

EXPERIMENTAL

Chemicals

All chemicals were reagent grade and used as received. Plants were grown in synthetic moderately hard reconstituted freshwater (MHRFW) as previously described [19] during treatments. Suwannee River Humic Acid Standard II was purchased from the International Humic Substances Society (IHSS, St. Paul, MN). *Egeria densa* was purchased from Nahackey's Aquarium (Melbourne, FL) in January 2015 and grown in reverse osmosis water for at least 2 days before testing.

Silver Nanoparticle Synthesis and Characterization

Silver nanoparticles were prepared according to a humic acid reduction of AgNO₃ [15]. Briefly, 1 L of humic acid solution (30 ppm) and 1 L AgNO₃ (1 mM) were heated in a sealed flask at 90°C for 1 hour. The nanoparticles were placed in the dark at ambient temperature for 24 hours. Nanoparticle concentration was estimated based the absorbance at 409 nm. Nanoparticle size was estimated according to Metz, et al. [20].

Plant Material and Metal Treatment

Silver nitrate was used to prepare 5, 10, 20, 30, 50, and 100 ppm Ag⁺ in MHRFW. A stock silver nanoparticle solution in MHSFW (30 ppm AgNps) was used to prepare silver nanoparticle treatment solutions at 5, 10, 20, and 30 ppm AgNps. Control solutions consisting of MHSFW and 15 ppm humic acid in MHSFW were prepared for the Ag⁺ and AgNps studies, respectively.

Stalks of *E. densa* (12 cm in length) were grown in test tubes filled with 50 ml of treatment solutions. Plants were grown in solution for 1 week in the Florida Institute of Technology greenhouse in February 2015. Temperature was maintained at approximately 25°C. Solution levels

were topped off with DI water every 2 days to ensure a constant volume of treatment solution.

Silver Analysis

After 1 week, plants were washed twice with DI water then dried at 120°C for 24 hours. Stalks were ground and dissolved in 70% HNO₃ overnight. Plants were digested according to Huang, et al., using a hot water bath in place of a microwave [21]. The concentration of silver was determined using flame atomic absorption (AA) spectroscopy. Total silver absorbed was normalized based on plant mass. Bioconcentration factors (BCF), which measure the absorption of a chemical compared to its concentration in the water column, were calculated based on the following equation: $BCF = (\text{silver absorbed in plant, ppm}) / (\text{silver in water, ppm})$ [22].

Statistics

All experiments were performed with five replicates. Data presented in figures represents the average \pm standard deviation. Significant differences were determined using Welch's analysis of variance (ANOVA), followed by pairwise comparisons using the Games-Howell Test (SPSS 23.0). Different letters in figures indicate statistically significant differences between treatments at $p < 0.05$. Pearson's product moment correlation (r) was used to determine relationships between silver exposures and silver absorption by *E. densa*, and significance was determined at $p < 0.05$. Log transformations were performed to normalize data that did not meet the assumptions of the statistical tests.

RESULTS & DISCUSSION

Analysis of Synthesized AgNps

An absorbance spectrum of the humic acid-reduced AgNps showed a peak at 415 nm and an absorbance of 1.17. This compared favorably to the spectrum reported by Akaighe [15]. The concentration of nanoparticles was determined to be 30 ppm with an average particle diameter of 30 nm. Thus, these particles can enter the cell through pores in the plasma membrane or by endocytosis, which involves the invagination of the plasma membrane

to absorb small particles and subsequent translocation throughout the cell [5].

Visual Analysis of Silver Species Toxicity

A decline in health was evident in plants exposed to silver in concentrations as low as 5 ppm. Plant health was

generally hindered at concentrations of 20 ppm Ag^+ and AgNps, as seen by the significant browning of the leaves in Figure 1. Higher concentrations of silver had a more pronounced effect on the plants for all measurements. Therefore, the presence of Ag^+ or AgNps caused an obvious decline in plant health over the exposure period.

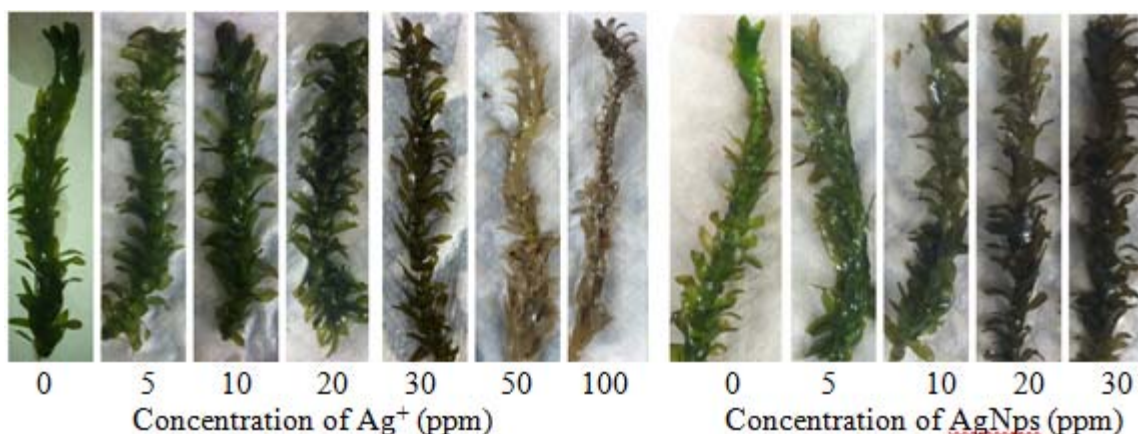


Fig 1. Phenotypic effects of silver treatments on *Egeria densa* 7 days after Ag^+ or AgNps treatments.

Similar phenotypes have been observed in related waterweeds such as *Elodea canadensis*, and have been linked to insufficient chlorophyll production by leaves (chlorosis) and cell death from toxic environments and extracellular factors (necrosis) [23, 24]. In these studies, 100 ppm lead exposures caused the leaves to turn brown and *E. canadensis* underwent chlorosis [23]. Similar effects were observed in the *E. densa* tests presented here with Ag^+ at 50 and 100 ppm. The plants underwent significant changes in color, resulting from silver toxicity which caused chlorosis and necrosis. Further, *E. densa* leaf tips began to turn brown at low concentrations of silver, indicating phytotoxicity to the photosynthetic apparatus and other subcellular components. As silver was absorbed, the *E. densa* withered and died. This is caused by an oxidative burst in the cell, resulting in lipid peroxidation, degradation of macromolecules, and other unfavorable reactions [5].

Silver Absorption Analysis

Previous research established that Ag^+ bioaccumulation occurs through sodium and copper ion transporters [5]. Once in the cells, Ag^+ can disrupt processes which normally regulate the introduction of

species through the cell wall. When these processes fail, more contaminants can enter the cell from the solution. This ultimately leads to cell death as demonstrated by the chlorotic and necrotic samples shown in Figure 1. Results of the silver cation flame absorption analysis are shown in Figure 2. *E. densa* exhibits a strong, positive correlation with a dose-dependent absorption of Ag^+ ($r=0.782$, $p<0.001$) over a 7-day exposure period. Rinsing plant samples in DI water following exposure to silver solutions removes any adsorbed silver species on the plant surface. Therefore, any silver detected by flame AA is due to silver found within the plant cells.

Results of the AgNps absorption study are shown in Figure 3. Absorbed silver increases with exposure to increasing concentrations of AgNps. (It should be pointed out that flame AA detects silver but does not distinguish between nanoparticles and cations released by the nanoparticles.) Like the Ag^+ results, the AgNps demonstrate a positive, dose-dependent increase in total silver absorption ($r=0.711$, $p<0.001$). Measurements of absorbed silver in the plant when exposed to 30 ppm AgNps solutions are statistically different compared to absorbed silver due to a 5 ppm solution. Solution concentrations of 10 and 20 ppm yield intermediate results. Comparisons of results for similar solution

concentrations for the two systems show no differences in absorbed silver ($p > 0.05$). This indicates that both Ag^+ and AgNps are absorbed to an equal extent by *E. densa*. Further, this similarity supports conclusions that the humic acid reduction of AgNO_3 produces AgNps which

are as toxic as Ag^+ at the same concentration. Concerns about ethical disposal of AgNps and Ag^+ -containing products are validated by these results.

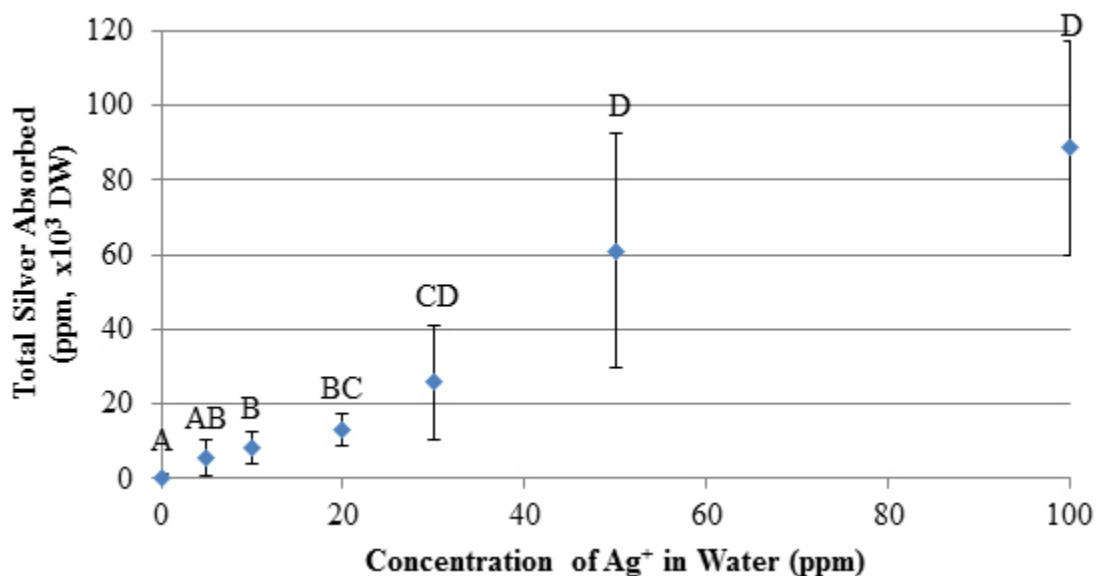


Fig 2. Total silver absorbed reported in mg/g dry weight. Each data point represents the mean \pm standard deviation ($n = 5$). Different letters indicate statistically significant differences between treatments at $p < 0.05$.

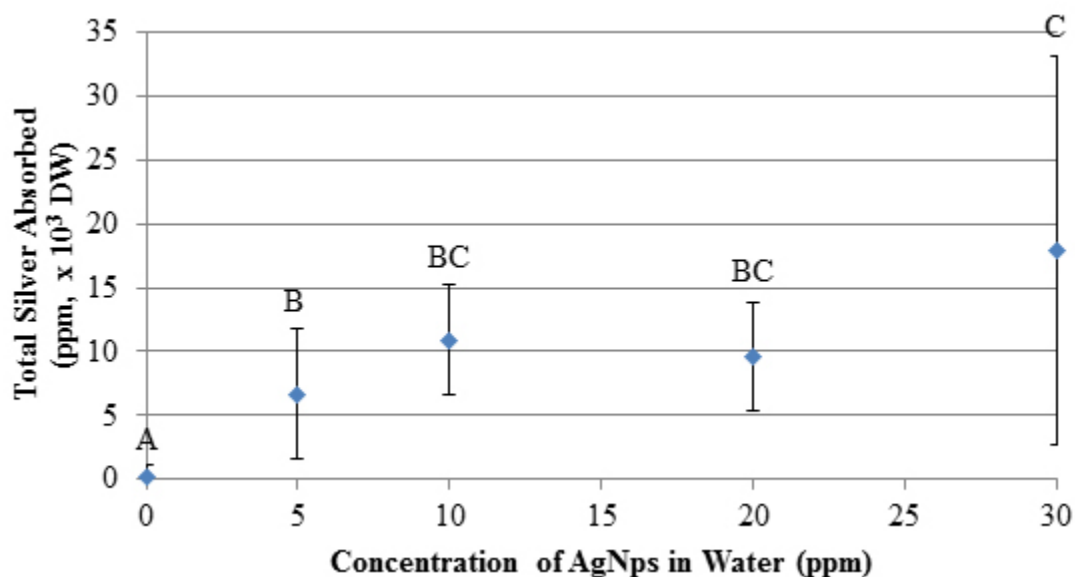


Fig 3. Total silver absorbed reported in mg/g dry weight. Data represents the mean \pm standard deviation ($n = 5$). Different letters indicate statistically significant differences between treatments at $p < 0.05$.

Bioconcentration Factor (BCF)

Bioconcentration factors can be compared between treatments to identify the maximum concentration of total silver species absorbed by *E. densa*. BCFs are a unitless ratio comparing the accumulation of a substance in an organism to its concentration in the environment [22]. BCFs vary widely between various substances including heavy metals. Some studies suggest that absorption of heavy metals can be time- and species-dependent, and that some plants are more viable for phytoremediation studies than others [25]. For example, in a 10 day study of mercury toxicity on *E. canadensis*, the BCF increased from 200 on day 2 to 580 on day 10 [22]. Duckweed (*Lemna gibba*) absorbed over significant amounts of Ag⁺ from solution at environmentally relevant concentrations, and is effective for phytoremediation of silver cations [26].

In this study, total silver species bioconcentration was measured, as shown in Table 1. High BCF values indicate that *E. densa* absorbed significant amounts of silver from its environment. The bioconcentration factors for the AgNps show a general decrease as concentration of AgNps in solution increases, whereas the Ag⁺ BCF is relatively constant. In both cases, silver species were absorbed into the plants. These BCF values of *E. densa* are reasonable compared to those in the literature.

There was a significant decline in BCF values for AgNps ($r=-0.56$, $p<0.001$) at higher AgNp concentrations. The amount of absorbed silver in plants at higher AgNp solution concentrations is greater than at lower concentrations but the amount absorbed does not increase proportionally to the AgNp solution concentration. The inability of silver to enter the plants at higher AgNp concentrations may be caused by some nanoparticles blocking the preferable adsorption sites on the surface of the plant. Alternatively, the nanoparticles could be involved in another step in the process of the plant's uptake of silver which has a rate that is independent of AgNp concentration. The significant decline in BCF for AgNps supports this, as plants exposed to 10-30 ppm AgNps showed no significant differences in total silver absorption (shown in Figure 3), suggesting that relatively fewer AgNps were absorbed by the plants when exposed to higher AgNp concentrations. The BCF values for Ag⁺ exposure were independent of Ag⁺ concentration ($p>0.05$), meaning that free Ag⁺ is readily absorbed by *E. densa* regardless of the concentration in solution, even after the plant shows severe signs of degradation at 50 and 100 ppm Ag⁺.

Table 1. Bioconcentration factors for *E. densa* after 7 day exposures to AgNps and Ag⁺. Different letters indicate significance at $p<0.05$. The designation n.s. represents non-significant differences ($p>0.05$).

Concentration of Silver in Water (ppm)	AgNps BCF	Ag ⁺ BCF
5	1334±658 ^a	1114±1015 ^{n.s.}
10	1091±470 ^{ab}	823±429 ^{n.s.}
20	480±208 ^b	648±209 ^{n.s.}
30	597±284 ^b	859±507 ^{n.s.}
50		1221±628 ^{n.s.}
100		887±286 ^{n.s.}

E. densa absorbs similar amounts of Ag⁺ and AgNps based on the bioconcentration factors of the two systems having the approximately the same values. Visual analysis of the plants suggests that like concentrations generally have the same effect on the plants. These results do not support one mechanism of silver toxicity over another, but clearly show that Ag⁺ and AgNps are both toxic to *E. densa*.

CONCLUSIONS

AgNps were successfully synthesized and characterized according to the humic acid reduction of silver nitrate. Visual effects of Ag⁺ and AgNps were observed at the end of a 7 day exposure of *E. densa*. Exposures to either silver cations or AgNps resulted in the bioaccumulation of silver within the plant cells and the amount of absorbed silver was proportional to the concentration in solution. Bioconcentration factors showed that plants absorbed significant amounts of silver species from the aqueous environment, indicating that *E. densa* is a viable candidate for phytoremediation of both types of silver.

These results are similar to studies involving other waterweeds, and demonstrate the negative effects of heavy metal pollutants on plants. Silver bioconcentration factors were of the same order of magnitude for both Ag⁺ and AgNps, but BCF declined at higher concentrations of AgNps while BCF of Ag⁺ remained constant. This suggests that the nanoparticles have a dependency on free Ag⁺ in the water. Further, the higher accumulation of Ag⁺ caused significant declines in physiological features and their

subsequent activities, indicating that silver species are toxic to *E. densa*.

Measurements of the total absorbed silver and BCF values indicate that *E. densa* can be used for effective phytoremediation of areas contaminated with silver species. Heavy metal contamination is a growing environmental concern, so successful removal using phytoremediation approaches with duckweeds and waterweeds should be studied further to provide an environmentally benign solution to remove toxins entering waterways. Additional studies can be performed using macrophytes and similar organisms (i.e. duckweeds) to determine which is most effective for silver species phytoremediation.

REFERENCES

1. Vance M, Kuiken T, Vejerano E, McGinnis S, Hochella M, Rejeski D, Hull M. *Beilstein J. Nanotechnol.*, 2015, 6, 1769-1780.
2. Ivask A, Kurvet I, Kasemets K, Blinova I, Aruoja V, Suppi S, Vija H, Kakinen A, Titma T, Heinlaan M, Visnapuu M, Koller D, Kisand V, Kahru A. *PLoS One*, 2014, 9, e102108.
3. Ellis LA, Valsami-Jones E, Lead JR, Baalousha M. *Sci. Total Environ.*, 2016, 568, 95-106.
4. United States Environmental Protection Agency Office of Water Regulations and Standards, Criteria and Standards Division, "Ambient Water Quality Criteria for Silver", Washington DC, 1980.
5. Fabrega J, Luoma SN, Tyler CR, Galloway TS, Lead JR. *Environ. Int.*, 2011, 37, 517-531.
6. Ratte H. *Environ. Toxicol. Chem.*, 1999, 18, 89-108.
7. Lapresta-Fernández A, Fernández A, Blasco J. *TrAC, Trends Anal. Chem.*, 2012, 32, 40-59.
8. Navarro E, Baun A, Behra R, Hartmann NB, Filser J, Miao A, Quigg A, Santschi PH, Sigg L. *Ecotoxicol.*, 2008, 17, 372-386.
9. Ravindran A, Chandrasekaran N, Mukherjee A. *Curr. Nanosci.*, 2012, 8, 141-149.
10. Oukarroum A, Barhoumi L, Pirastru L, Dewez D. *Environ. Toxicol. Chem.*, 2013, 32, 902-907.
11. Mazumdar H. *Int. J. Eng. Sci.*, 2014, 4, 12-20.
12. Wigginton NS, De Titta A, Piccapietra F, Dobias JAN, Nesatyy VJ, Suter MJF, Bernier-Latmani R. *Environ. Sci. Technol.*, 2010, 44, 2163-2168.
13. Rahman MA, Hasegawa H. *Chemosphere*, 2011, 83, 633-646.
14. Akaighe N, MacCuspie RI, Navarro DA, Aga DS, Banerjee S, Sohn M, Sharma VK. *Environ. Sci. Technol.*, 2011, 45, 3895-3901.
15. Akaighe N, Depner SW, Banerjee S, Sohn M. *Chemosphere*, 2013, 92, 406-412.
16. Gao J, Youn S, Hovsepian A, Llaneza VL, Wang Y, Bitton G, Bonzongo JJ. *Environ. Sci. Tech.*, 2009, 43, 3322-3328.
17. Hawley GG, Lewis RJ Sr in *Hawley's Condensed Chemical Dictionary: Humic Acids*, Wiley, Hoboken, NJ, 2007.
18. Perdue, EM in *Functions of Natural Organic Matter in Changing Environment: Standard and Reference Samples of Humic Acids, Fulvic Acids, and Natural Organic Matter from the Suwannee River, Georgia: Thirty Years of Isolation And Characterization*, ed Xu, J, Zhejiang University Press and Springer Science+Business Media, Dordrech, 2013, pp 85-88.
19. United States Environmental Protection Agency Office of Water, "Methods for Measuring the Acute Toxicity of Effluents and Receiving Waters to Freshwater and Marine Organisms", Washington DC, 2002.
20. Metz K, Sanders S, Miller A, French K. *J. Chem. Educ.*, 2014, 91, 264-268.
21. Huang L, Bell RW, Dell B, Woodward J. *Commun. Soil Sci. Plant Anal.*, 2004, 35, 427-440.
22. Lewis MA, Wang W in *Plants for Environmental Studies: Metal Accumulation by Aquatic Plants*, eds Wang, Lower, Gorsuch, Hughes, 2010, CRC Press, Boca Raton.
23. Dogan M, Saygideger SD, Colak U. *Bull. Environ. Contam. Toxicol.*, 2009, 83, 249-254.
24. Malec P, Maleva M, Prasad MNV, Strzałka K. *Bull. Environ. Contam. Toxicol.*, 2009, 82, 627-632.
25. Abu Bakar AF, Yusoff I, Fatt NT, Othman F, Ashraf MA. *BioMed Res. Int.*, 2013, 2013, 1-7.
26. Sasmaz A, Obek E. *Chem. Erde Geochem.*, 2012, 72, 149-152.



Antifungal Activity of Silver Loaded Zeolite A from Bagasse Ash against *Candida Albicans*

Alfa A. Widati*, Afaf Baktir, Ryan Rachmawan

Dept. of Chemistry, Faculty of Sci. & Technology, Universitas Airlangga, Surabaya 60115 Indonesia

(*E-mail: alfaakustia@fst.unair.ac.id)

Abstract: Normally, *Candida albicans* is found in the gastrointestinal tract, the upper respiratory tract and the genital mucosa of mammals. *Candida albicans* can form biofilm because of the increasing population and the resistance of the existing antifungal. Silver loaded zeolite A is an anti-fungal material that is effective in inhibiting the pathogen microorganism. This study aims to demonstrate the preparation of silver loaded zeolite A from bagasse ash and its antifungal activity against *Candida albicans*. Silver loaded zeolite A was obtained by ion exchange mechanism on zeolite A. It was characterized using XRD and XRF. The inhibition of the growth of *Candida albicans* by silver loaded zeolite A was observed from cell viability of *Candida albicans*. The optimum concentration of silver loaded zeolite A to inhibit the growth of *Candida albicans* was 4.5 g/L at 60 hours. This inhibition mechanism was resulted from the releasing of silver from zeolite A.

Key Words: *Candida albicans*, silver loaded zeolite A, bagasse ash, viability cell, antifungal

INTRODUCTION

Candida albicans is a normal flora found in respiratory, gastrointestinal tract, mucous membranes, vagina, urethra, and skin. If the immune system becomes compromised, *Candida albicans* can infiltrate the bloodstream and diffuse to organs such as kidney, heart and brain [1]. Several diseases caused by *Candida albicans* are vulvaginistis candiduria, gastrointestinal candidiasis that can cause gastric ulcers and cancer [2]. *Candida albicans* forms biofilms due to an overdose of antifungal consumption [3]. Biofilms as a *Candida albicans* protection cause the body to exhibit toward immune system and antifungal agents. Biofilms can absorb the nutrients of the host cell therefore promote the growth colonies. The growth of biofilms is along with the increase of clinical infection in the host cell.

Fungal infections can be treated with the proper use of antifungal agents. The use of antifungal agents should be accompanied by caution for the dangers of biofilm resistance. A new of antifungal substance is needed to prevent this effect. Therefore, It is necessary to conduct research to develop a new antifungal which is more effective against clinical disease mainly caused by bacteria, fungi or virus. One effort to develop new antifungal agents

is the using of zeolite as an unique, cheap, and easy to synthesize material. Zeolite as a molecular sieves has been used for membranes, catalysts, and ion exchange [4-5]. Zeolite also has been used in the biomedical field as detoxifier, decontaminant, antibacterial, drug screen, biosensors and anti-tumour [6].

Zeolite clinoptilolite and zeolite A are widely used in the biomedical field [7-8]. Unfortunately, zeolite clinoptilolite as a zeolite has impurities such as montmorillonite, apatite, quartz, oxide of Ca, Al, Si, Fe, and other elements [9]. The presence of impurities can affect to the activity of zeolite and also impact the negative effects on health. On the contrary, zeolite A is an antifungal material that is safe, nonteratogenic agent, and it does not induce toxicity and carcinogenicity. The antifungal ability of zeolite A has been reported in previous studies [10-11]. The studies demonstrated that the activity of zeolite A against *Acinetobacter junii* with EC_{50} is 0.138 to 0.328 g/L, *Saccaromyces cereviceae* with EC_{50} is 2.88 to 5.47 g/L, *Ceriodaphnia dubia* with EC_{50} is 0.425 g/L [10]. Antifungal ability of zeolite A results generation hydroxyl ions during hydrolysis. The hydroxyl ions will increase the release of silicon and aluminium from zeolite framework and formed positively charged complex $[Al_mH_nNa_pO_qSi_{3-5}]^{2+}$ or $[(NaOH)_x(AlO(OH))_y(Si(OH)_4)_3-5]^{2+}$. The positively charged complex will interact with the

electronegative cell walls of microbes (phosphoryl, carboxyl, and hydroxyl) through electrostatic interaction [10].

Meanwhile, silver is also an antifungal agent that is effective to inhibit the pathogenic microorganisms such as virus, bacteria and eukaryotic microorganisms [12]. The antifungal activity of silver is effective against about 650 types of bacteria. Silver ions can provide antifungal effects at low concentrations [13]. Submillimolar concentration of AgNO_3 is lethal to gram-negative and gram-positive bacteria. In this paper, we present a preparation of zeolite A from bagasse ash, modification of preparation zeolite using silver, and investigation of the antifungal activity of silver loaded zeolite A against *Candida albicans*. This research also utilized the waste of sugar industry through the using of bagasse ash as a source of silica in the synthesis of zeolite A.

EXPERIMENTAL SECTION

Materials and Instruments

In this study, bagasse were obtained from Sugar Company Candi Baru Sidoarjo, Indonesia. All of chemicals were analytical grade and used as received without further purification, sodium aluminate (Sigma Aldrich), hydrochloric acid (Merck), sodium hydroxide (Merck), silver nitrate (Merck), tetrazolium XTT (Biomedicals), menadione (Sigma Aldrich), and Difco Yeast Extract (Merck). The instruments used were an autoclave (OSK 6508 Steam Pressure Apparatus Ogawa Seiki Co.,Ltd.), centrifuge (Universal 320R Zentrifugen), laminair air flow cabinet (Kotterman 8580), X-ray diffraction (JEOL JDX-3530, Philips), X-ray fluorescence (JEOL JSX 3400R, Philips), and UV-Vis spectrophotometer (Pharmaspec UV-1700, Shimadzu).

Methods

Synthesis of amorphous silica from bagasse

The procedure of synthesis of amorphous silica from bagasse ash was adopted from the previous method [14]. Amorphous silica was synthesized using dried bagasse. Bagasse was dried in an oven at 190°C for 1 hour. The dried bagasse was calcined at 300°C for 30 minutes and continued at 600°C for 60 minutes for ashing process. The resulting ash was then characterized using XRD to evaluate the formation of amorphous silica.

Bagasse ash was placed into a beaker and poured with hot water. Then, concentrated HCl was poured on it and evaporated. This treatment was repeated three times. Furthermore, the mixture was poured into water and concentrated HCl (20:1 v/v) in water bath for 5 minutes. The mixture was then filtered and washed 4-5 times with hot water. The resulted powder was calcined at 300 °C for 30 minutes, followed at 600 °C for 1 hour to produce the amorphous silica. Sample was characterized by XRF to determine the concentration of silica.

Synthesis of zeolite A from bagasse ash

Zeolite A was synthesized based on the previous research with the molar composition was $3.9 \text{ Na}_2\text{O}:1\text{Al}_2\text{O}_3:1.8 \text{ SiO}_2:270 \text{ H}_2\text{O}$ [15]. The gel was prepared using aluminate and silicate precursor solution. The precursor solution of aluminate was prepared by dissolving NaAlO_2 in NaOH solution. The precursor solution of silicate was prepared by dissolving SiO_2 in NaOH solution. Both of precursor solution was combined under vigorous stirring. The mixture was heated at 100 °C for 12 hours. After/that, the mixture was filtered, washed, dried, and calcined at 450 °C for 4 hours. The solid zeolite A was then characterized using XRD.

Synthesis of silver loaded zeolite A

The silver loaded zeolite A was synthesized based in the previous method [16]. 1.5 g of zeolite was combined with 10 mL of 0.05M, AgNO_3 . The mixture was stirred and heated at 80 °C for 2 hours and dried at 100°C for 24 hours. The dried mixture was calcined at a temperature of 450 °C for 4 hours. Silver loaded zeolite A were characterized using XRF to determine the amount of silver ions.

Study of antifungal activity of silver loaded zeolite A against Candida albicans

Before being used for testing antimicrobial activity against *Candida albicans*, silver loaded zeolite A was sterilized by drying at 105 °C for 16 hours. Silver loaded zeolite A was added to 100 mL of distilled water with stirring at 30 °C for 24 hours. The suspension was used in an antifungal test against *Candida albicans* [16]. The liquid medium of *Candida albicans*, YPD was prepared by combining peptone, dextrose, and yeast extract in aquades. The mixture was sterilized at 121°C for 15 minutes and stored at cold temperature.

The test of antifungal activity was done by adding 0.25 mL of inoculum *Candida albicans* in 5 mL YPD liquid medium that contained silver loaded zeolite A with variation of concentrations (0 to 4.5 g/L). The suspension was incubated at 37 °C and shaken as a function (0 to 60 hours). The growth of *Candida albicans* was determined by cell viability. Through this method, the concentration and the optimum time of silver loaded zeolite A to inhibit the growth of *Candida albicans* can be determined.

Analysis of cell viability

Candida albicans was suspended in 3 mL of phosphate buffer saline (PBS) and which was added with 50 mL of XTT solution and 8 mL of menadione. Then, it was incubated at 37 °C for 4 hours in the dark room and centrifugated at 2000 rpm for 15 minutes. The resulting supernatant was measured for absorbance using Spectrophotometer UV-Vis at 469 nm.

RESULTS & DISCUSSION

Amorphous Silica from Bagasse Ash

Two basic process in the synthesis of amorphous silica from bagasse are drying and calcinations. Drying occurs when heating bagasse at 190 °C for 1 hour to remove water in in the materials. The presence of water in the bagasse affects the purity of sugarcane bagasse. The calcination is done at 300 °C for 30 minutes to convert bagasse into carbon. The next calcination step is heated at 600 °C for 60 minutes to remove carbon so that white ash of silica is obtained. White ash is purified by washing using hydrochloric acid to dissolves oxides of metals such as P₂O₅, K₂O, MgO, Na₂O, CaO, dan Fe₂O₃ to form chloride salts [17]. The diffractogram of amorphous silica from bagasse ash is shown in Figure 1. It can be seen that there is a hump in 2θ 15-35°. According to the literature [18], a hump is observed in the 2θ ranging from 16° to 39°, indicating disordered structure. Herein, a hump from the prepared solid which supposed to be the characteristic of amorphous silica. The same results were also reported by Malek and Yusof [19-20], which displayed the hump at 2θ 15-30° with a peak at 23° when calcined the rice husk and bagasse at high temperatures. Based on analysis result of XRF, the amount of silica in the bagasse ash obtained is about 88.7%. Moreover, this data was applied as a basic of calculation in the synthesis of zeolite A with molar composition 3.9 Na₂O: Al₂O₃: 1.8 SiO₂ · 270 H₂O.

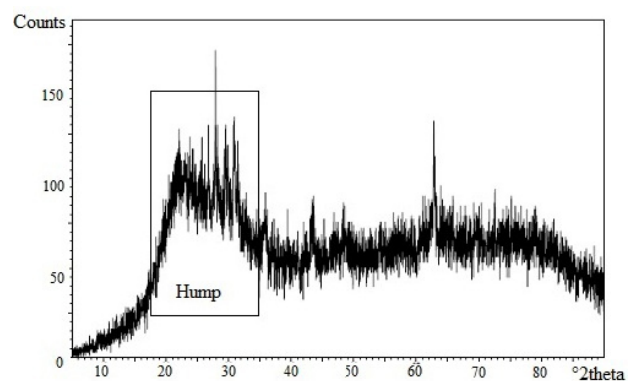


Fig 1. The diffractogram of amorphous silica from bagasse ash

Silver Loaded Zeolite A from Bagasse Ash

Synthesis of zeolites using the hydrothermal method involve a crystallization process of solution through heating and high pressure in water solvent. Water is used as a media for transformation of amorphous into a crystalline solid. The hydrothermal process requires a relatively low temperature to prevent changes in the structure of the zeolite A. According to the literature, zeolite A can be transformed into another structure at high temperatures, so the temperature is one of important factor in the synthesis process [21]. High purity of zeolite A is obtained at hydrothermal temperatures of 100 °C for 12 hours [19]. The structure of zeolite A was analyzed using XRD. The diffractogram shows the intensive peak at 2θ = 14.26; 24.87; 32.36; 35.49; 38.48; and 43.90°. In this study, the structure of zeolite A is crystalline for stable form when applied as an antifungal material.

Silver loaded zeolite A was prepared by mixing zeolite A, and a solution of 0.05M, AgNO₃. The ions of silver exchange the position of sodium ions in zeolite A framework. From the results of XRD analysis, it can be seen that there is a decreasing of peak intensity at 2θ 14.26; 24.87; 32.36; 35.49; 38.48; and 43.90°. In the silver loaded-zeolite A, the diffractogram indicates the presence of silver that is proved by peak at 2θ 38.10 and 44.24°. That peaks also represented the (111) and (200) hkl as Bragg's reflection of face centered cubic crystalline silver. The pattern of diffractogram is similar with the previous report [22]. The addition amount of Ag in the zeolite A leads to a decrease in the amount of silica because the collapsed structure of zeolite. XRD pattern of zeolite A and silver loaded zeolite A from bagasse ash shown in Figure 2.

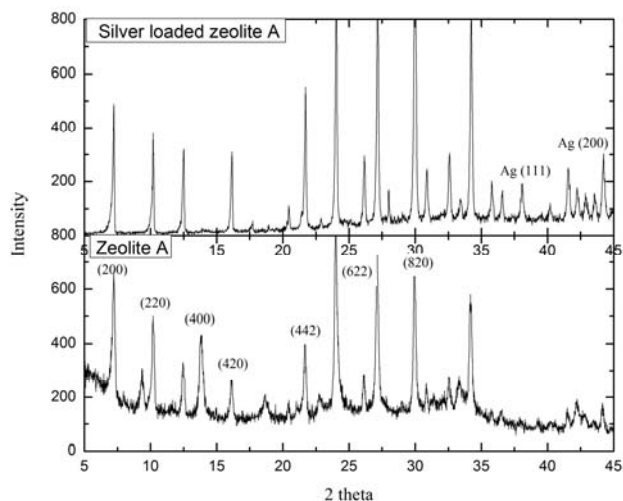


Fig 2. The diffractogram of (a) zeolite A from bagasse ash (b) silver loaded zeolite A from bagasse ash

Antifungal Activity of Silver Loaded Zeolite A against *Candida Albicans*

The influence of silver loaded zeolite A on the growth of *Candida albicans* is obtained through determination of cell viability using spectrophotometer UV-Vis at 469 nm. This analysis is based on the reducing ability of active cell metabolism towards XTT into a formazan orange with the presence of the dehydrogenase enzyme of mitochondria and menadione. The dehydrogenase enzyme of mitochondria is an oxidizing agent, thereby converting NADH into NAD⁺ and H⁺ by releasing electrons. Dehydrogenase enzyme consists of three kinds of complex enzymes (NADH-Q reductase, cytochrome reductase, and cytochrome oxidase). The presence of dehydrogenase enzyme of mitochondria can be an indicator of living cells. In contrast, dehydrogenase enzyme does not work in the death cell.

XTT is not soluble in lipids so that it can not diffuse through the membrane. Therefore, in cell viability tests, menadione is needed as a media for the XTT to diffuses to mitochondria through cell membranes. Menadione acts as an electron carrier that is soluble in lipid. Dehydrogenase enzymes of mitochondrial reduced menadione into menadiol and generated NADH. Furthermore, menadiol diffuse out of the cell membrane and reacts with XTT, forms colored formazon compound [23-24]. The intensity of the colored formazan is analogue with the number of surviving cells.

The profile of *Candida albicans* growth is influenced by the concentration of silver loaded zeolite A (0 to 4.5 g/L), as shown in Figure 3. The growth profile consists of four phases: lag, exponential, and a death phase. Lag phase is an adaptation phase that occur when the population of *Candida albicans* is inoculated into a new medium. Exponential phase is a phase which at *Candida albicans* reproduces by itself. Death phase (lysis) is a phase of decreasing the number of *Candida albicans* due to nutritional deficiencies or unsupported medium.

There are three phases of growth profile in the control media (0 g/L) and in the concentration of silver loaded zeolite A 1.5 and 3 g/L. They are lag exponential, and death phase. Lag phase occurs in the 0 to 12 hours, whereas exponential phase occurs at 12 to 36 hours, and death phase occurs after 36 hours. In the concentration of silver loaded zeolite A 4.5 g/L, one phases of growth profile was obtained, death phase. The formation of biofilm was occurred at 48 and 60 hours in the control medium (0 g/L).

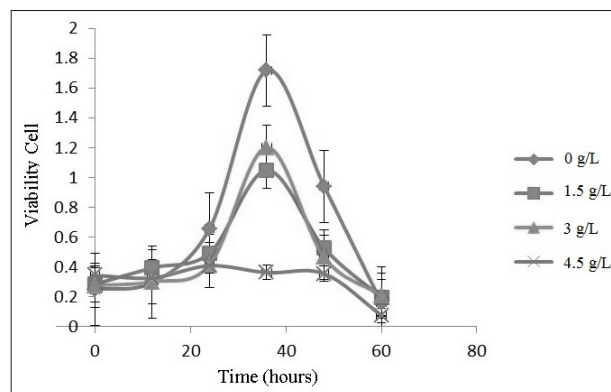


Fig 3. The growth profile of *Candida albicans* with the addition of silver loaded zeolite A. Determination of the growth profile is done in YPD medium for 60 hours with various concentrations of silver loaded zeolite A

The graph indicates that the silver loaded zeolite A is able to inhibit the growth of *Candida albicans*. The greater the concentration of silver loaded zeolite A, the larger inhibitory activity against *Candida albicans*. The mechanism of inhibition is due to the releasing of silver ions from zeolite A. Table 1 presents the amount of silver ion that release from zeolite framework. The silver ion inhibited cellular respiration system and binded with

sulphydrals enzyme, therefore destroyed the protein bonds [25-27]. Therefore, the optical density is decreased, the amount of the growth of *Candida albicans* should also be decreased.

Table 1. The concentration of releasing silver ion from zeolite A framework based on analysis of AAS

Mass of silver loaded zeolite A	Concentration of silver ion (%)
1.5 g/L	3.860
3 g/L	5.782
4.5 g/L	7.854

From the results of antifungal activity of silver loaded zeolite A with various concentration, it concluded that silver loaded zeolite A with a concentration of 4.5 g/L is an optimum concentration to inhibit the growth of *Candida albicans*. In this condition, the concentration of silver is 1.8 mg/L. Meanwhile, the occupational exposure limit for silver ion is 10 mg/L [28]. Therefore, silver loaded zeolite A potential to apply in manufacturing of medicine, medical devices, household items, and textiles where antifungal properties are required.

Despite of the mechanism of silver ions releasing, the inhibition mechanism *Candida albicans* is also due to hydroxyl ions that are produced by zeolite A due to hydrolysis, resulting higher pH. Hrenovic et al. [10] has studied this phenomenon. The possible reaction of generating of hydroxyl ions from zeolite is:



In this research, the pH of water is increased respectively 7.33 to 5.84 on zeolite concentration of 1.5 g/L; 5.89 becomes 7.84 on zeolite concentration of 3 g/L; and 6.01 to 8.47 at a concentration of zeolite 4.5 g/L. The greater the silver loaded zeolite A concentration, the higher the media basicity (Figure 4). According to the previous research [10], the hydroxyl ions will increase the release of silicon and aluminum from the zeolite framework forming positively charged complex $[Al_mH_nNa_pO_qSi_{3-5}]^{2+}$ or $[(NaOH)_x(AlO(OH))_y(Si(OH)_4)_{3-5}]^{2+}$. When *Candida albicans* is planktonic, the positively charged complex will interact with the electronegative cell membrane of microbes, such as phosphoryl, carboxyl, and hydroxyl through electrostatic forces.

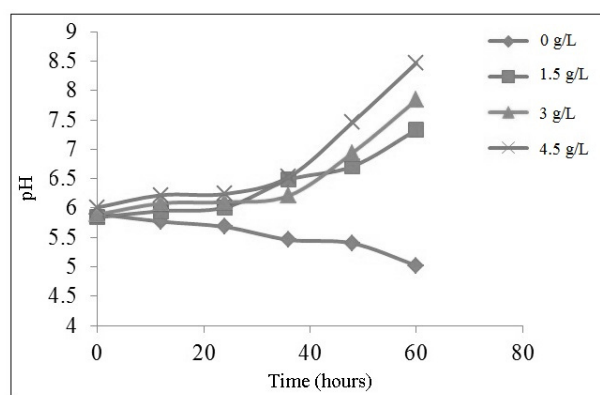


Fig 4. The pH of YPD media contains various concentrations of silver loaded zeolite A

Moreover, the alkalinity is not a major factor in inhibiting the growth of *Candida albicans*. At 36 hours, all of media generate a similar pH but different value of the cell viability. It can be concluded that the amount of released silver ions has a more substantive role than hydroxyl ions to inhibit the growth of *Candida albicans*.

CONCLUSION

This study successfully synthesized silver loaded zeolite A from bagasse through ion exchange mechanism. Silver loaded zeolite A has antifungal activity against *Candida albicans* through the release mechanism of silver ions. The optimum concentration of silver loaded zeolite A in inhibiting the growth of *Candida albicans* is 4.5 g/L at the optimum time of 60 hours. The use of silver loaded zeolite A with this concentration is appropriate for the use in manufacturing of medicine, medical devices and other industries that required the antifungal properties.

ACKNOWLEDGMENT

The authors would like to show appreciation to the Department of Chemistry, Faculty of Science and Technology, Universitas Airlangga for the use of laboratory facilities. The authors would also like to express gratitude to Prof. Dr. Afaf Baktir, MS for the guidance during the research.

REFERENCES

1. Nett J, Andes, *Microbiology*, 2006, 9, 1-6.
2. Rintiswati N, Praseno, Setyawan I, Suharyono, *Periodic Medical Sciences*, 2003, 35(1), 17-22.
3. Jin Y, Samaranyake LP, Samaranyake Y, Yip HK, *Archive of Oral Biology*, 2004, 49, 789-798.
4. Flanigen EM, *Pure Applied Chemistry*, 1980, 52, 2191-2211.
5. Barthomeuf D, *Catalysis Review*, 1996, 38, 521-612.
6. Auerbach SM, Carrad KA, Dutta PK, *Handbook of Zeolite Science and Technology*, Marcel Dekker Inc., 2003.
7. Cerri G, De'Gennaro M, Bonferoni M, Caramella C, *Applied Clay Science*, 2004, 27, 141-150.
8. Rodriguez-Fuentes G, Barrios MA, Iraizoz A, Perdomo I, Cedre B, *Zeolites*, 1997, 19, 441-448.
9. Estiaty LM, Fatima D, presented at the Exposure Research awl-LIPI Geotechnology-Indonesia, 2009, ISBN: 978-979-8636-16-5.
10. Hrenović J, Željezić D, Kopjar N, Sarpola A, Bronić J, Sekovanić L, *Journal of Hazardous Materials*, 2010, 183, 655-663.
11. Warne MStJ, Schifko AD, *Ecotoxicology and Environmental Safety*, 1999, 44, 196-206.
12. Yaohui L, Liu H, Wang Z, Hao L, Zhan J, *Polymer for Advanced Technologies*, 2008, 19, 1455-1460.
13. Lee S, Kim H, Patel R, Joon Im S, Kim J, Min B, *Polymer for Advanced Technologies*, 2007, 18, 562-568.
14. Wibowo, *Journal of Civil Engineering*, 2006, 6(2), 124-136.
15. Pera-Titus M, Bausach M, Liorens J, Cunill F, *Separation and Purification Technology*, 2008, 59(2), 141-150.
16. Rivera-Garza M, Olguin MT, Garcia-Sosa I, Alcantara D, Rodriguez F, *Microporous and Mesoporous Materials*, 2002, 39, 431- 444.
17. Yalcin N, Sevinc V, *Ceramic International*, 2001, 27, 219-224.
18. Singh D, Kumar R, Kumar A, Rai KN, *Ceràmica*, 2008, 54, 203-213.
19. Malek NA, Yusof AM, *The Malaysian Journal of Analytical Sciences*, 2007, 11(1), 76-83.
20. Sompech S, Dasri T, Taomola S, *Oriental Journal of Chemistry*, 2016, 32(4), 1923-1928.
21. Perego C, *Catalyst Today*, 1997, 34, 281-305.
22. Cheng Hsin-Han H, Chu-chin, Tsai Chia-His, *Aerosol and Air Quality Research*, 2012, 12, 409-419.
23. Stryer L, Berg JM, Tymoczko JL, *Biochemistry*, 7th Edition, New York: WHFreeman and Company, 2012;
24. Rabinowitz JD, Vacchino JF, Beeson C, McConnell MH, *American Chemical Society*, 1997, 120(10), 2464-2473.
25. Matsumura Y, Yoshikata K, Kunisaki S, Tsuchido T, *Applied and Environmental Microbiology*, 2003, 69(7), 4278-4281.
26. Russell AD, Hugo WB, *Progress in Medicinal Chemistry*, 31, 351-370.
27. Matsuura T, Abe Y, Sato Y, Okamoto K, Ueshige M, Akagawa Y, *Journal of Dentistry*, 1997, 25(5), 373-377.
28. Drake PL, Hazelwood KJ, *The Annals of Occupational Hygiene*, 2005, 49(7), 575-585.



3-Bromopyruvate and Genistein Combination Inhibits Glycolysis and Induces Cell Death in DU-145 and LNCaP Prostate Cancer Cells

Harris Goldsmith¹, Gintare Kazdailyte², James Kwasi Kumi-Diaka^{1*}

¹ Department of Biological Sciences, College of Science, Florida Atlantic University, Florida, USA

² University of Skovde, Sweden

(*E-mail: jdiaka@fau.edu)

Abstract: Prostate cancer is among the leading cancer-related causes of death in United States. An estimated 161,360 new cases and 26,730 cancer related deaths are expected in 2017. Conventional therapeutics flaws/short-comings include side effects which could be long-lasting and fatal. Current research is focused on attacking cancer cells by inhibiting signaling pathways in carcinogenesis, and finding molecular targets for potential therapeutic molecules. The long-term goal/objective of our study/project is to determine the efficacy of 3-Bromopyruvate (3BP)-Genistein (Gn) combination treatment to target glycolysis and induce cell death in LNCaP and DU-145 prostate cancer cells, at significantly lower concentrations while minimizing or eliminating potential side effects. Data from the preliminary studies revealed that: i) genistein significantly potentiates the treatment-induced apoptotic cell death of 3-bromopyruvate in both cancer cell lines; the mechanism of growth inhibition included targeting the energy metabolic pathways of the cells.

Key Words: - Prostate cancer cell lines; 3-bromopyruvate; Genistein isoflavone; 3BP-Gn combination therapy.

RESEARCH COMMUNICATION

Prostate cancer is one of the most common cancers found in American men, becoming the second leading cause of cancer related deaths in the United States of America. An estimated 161,360 new cases and 26,730 cancer related deaths are expected in the year of 2017 [1]. Conventional chemotherapy is flawed by induction of side effects which could be long-lasting and fatal. Developing alternative therapeutic treatments is an ongoing focus in research. Current researches are focusing on attacking cancer cells by inhibiting signaling pathways in carcinogenesis, inducing apoptosis molecules and growth inhibitors. The long-term goal/objective of our study/project is to determine the efficacy of 3-Bromopyruvate (3BP)-Genistein (Gn) combination treatment to target glycolysis and induce cell death in LNCaP and DU-145 prostate cancer cells, at significantly lower concentrations while minimizing or eliminating potential side effects.

In this study, LNCaP and DU-145 prostate cancer cells were incubated under humidified atmosphere at 37°C and CO₂ for 48 hr to achieve +80% confluence in 96-well microtiter plates (96 well-MTP). The cells were then exposed to varying concentrations of 3BP (3BP_{60-160 μM}) and 3BP + genistein (3BP_{60-160 μM} + Gen₆₀), incubated for 48-72 hr and then analyzed/assayed using 3-(4, 5-dimethylthiazol-2-yl)-2, 5-diphenyltetrazolium bromide (MTT) and Nitroblue tetrazolium (NBT) reagents. MTT assay was used to evaluate the cells' metabolic activity (treatment-induced cell death); Nitroblue tetrazolium assay (NBT) was used to assess treatment-induced intracellular ROS levels (and correlate this with cell death); and fluorescence microscopy was used to analyse and assess the kind/types of treatment-induced cell death (percentage apoptosis vs percentage necrosis).

The preliminary data revealed that: i) both treatment regimen (3BP and 3BP-Gn combination) induced cell death (apoptosis and necrosis) in both cancer cells; ii) treatment-induced cell death was concentration-dependent; the percentage cell death increased

concomitant with increasing concentration of both drug treatments (3BP and 3BP-Gn combination); iii) percentage cell death at each dosage level was significantly higher ($P < 0.001$) in the 3BP-Gn combination ($3BP_{60-100 \mu M} + Gen_{60}$) compared to the single 3BP treatment; iv) the NBT assay showed a dose-dependent decrease of ROS levels produced in both treatments while the 3BP-genistein combination treatment had higher levels of ROS induction compared to single 3BP treatment; v) treatment-induced apoptosis correlated with treatment-induced ROS levels.

In general, the data obtained in this study are in conformity with reports of previous studies which reported treatment-induced apoptotic cell death in cancer cells exposed to genistein or 3-bromo-pyruvate [2,3,4]. Unique aspects of cancer cells include their ability to alter their energy metabolism and evade cell death. These bioenergetic features allow the cancer cells to survive hypoxic conditions and enable their proliferation and invasiveness [5,6]. While normal cells produce most of their energy through mitochondrial respiration, cancer cells exhibit the "Warburg Effect", in which the cellular energy, adenosine triphosphate (ATP) production, is derived from aerobic glycolysis resulting in lactic acid production [3,7,8,9]. Furthermore, steady-state ROS balance is high in cancer cells versus normal cells, where increased persistent ROS may cause oxidative damage to DNA of cancer cells and initiation of apoptosis, suggesting that a delicate balance of intracellular ROS is required for cancer cell function [2, 3].

In cancer cells, high levels of ROS can result from increased metabolic activity, mitochondrial dysfunction, and increased activity of oxidases [2]. Consequently, targeting these signaling pathways via increasing intracellular ROS may reduce stimulation of glucose uptake and inhibit glycolysis. This can have many therapeutic implications such as depleting the cancer cell of bioenergy (ATP), inhibiting cell proliferation and consequent cell death. 3BP treated cells revealed 55% increased intracellular ROS production compared to control [10].

Genistein has been reported to have increased intracellular ROS at higher concentrations ($>50 \mu M$) [11]. Genistein isoflavone (genistein - 4',5,7-trihydroxyisoflavone) is a small molecule found in soy that has been found to possess potent anti-cancer activities [12]. In a study done by Gerhauser, genistein treatment of pancreatic cancer cells inhibited hexokinase, which is an important mediator of glycolysis [13].

In another study, Pavese discovered that genistein was able to decrease metastatic formation by inhibiting prostate cancer cell detachment and invasion [14,15]. These studies augment the potential significance of genistein in formulating treatment regimens for cancer prevention and/or treatment. Our data showed that genistein potentiates the anti-cancer activity of 3-bromopyruvate in a dose-dependent manner, indicating the potential therapeutic significance of the combination regimen. In-depth studies are in progress to delineate the signaling pathways and therapeutic targets/markers for the 3BP-Gn combination regimen in prostate cancer lines in vitro and in vivo.

REFERENCES

1. American Cancer Society. Prostate Cancer. American Cancer Society, Atlanta, USA, 2016, pp 1-5.
2. Speirs CK, Hwang M, Kim S, Li W, Chang S, Varki V, Lu B. Harnessing the cell death pathway for targeted cancer treatment. *Am. J. Cancer Res.*, 2011, 43-61.
3. Dakubo GD in *The Warburg Phenomenon and Other Metabolic Alterations of Cancer Cells*, Springer Berlin, Heidelberg, 2010, pp 39-66.
4. Bensinger S, Christofk H. New Aspects of the Warburg effect in cancer cell biology. *Elsevier*, 2012, 352-359.
5. Lee M, Yoon J. Metabolic interplay between glycolysis and mitochondrial oxidation: The reverse Warburg effect and its therapeutic implication. *World J. Biol. Chem.*, 2015, 148-161.
6. Pelicano H, Martin DS, Xu R-H, Huang P. Glycolysis inhibition for anticancer treatment. *Oncogene*, 2006, 4633-4646.
7. Su Z, Yang Z, Xu Y, Chen Y, Yu Q. Apoptosis, autophagy, necroptosis, and cancer metastasis. *Molec. Cancer*, 2015, 1-14.
8. Kumi-Diaka J, Oseni S, Famuyiwa T, Branly R. Therapeutic Impact of Vitamin C on the Anticancer Activities of Genistein Isoflavone in Radiosensitized LNCaP Prostate Cancer Cells. *J. Cancer Prev. Curr. Res.*, 2015, 2-7.
9. Chiyomaru T, Yamamura S, Fukuhara S, Yoshino H, Kinoshita T, Majid S, Saini S, Chang I, Tanaka Y, Enokida H, Seki N, Nakagawa M, Dahiya R. Genistein Inhibits Prostate Cancer Cell Growth by Targeting miR 34a and Oncogenic HOTAIR. *PMC*, 2013, 1-10.
10. Melissa McCracken, Miho Olsen, Moon S. Chen Jr., Ahmedin Jemal, Michael Thun, Vilma Cokkinides, Dennis Deapen, Elizabeth Ward. Cancer incidence,

- mortality, and associated risk factors among Asian Americans of Chinese, Filipino, Vietnamese, Korean, and Japanese ethnicities. *Ca-Cancer J. Clin.*, 2007, 57, 190-205.
11. Jagadeesh S, Kyo S, Banerjee P. Genistein Represses Telomerase Activity via Both Transcriptional and Posttranslational Mechanisms in Human Prostate Cancer Cells. *Cancer Res*, 2006, 2107-2115.
 12. Li Y, Sarkar F. Inhibition of Nuclear Factor KB Activation in PC3 Cells by Genistein is mediated via Akt Signaling Pathway. *Cancer Res.*, 2002, 2369-2377.
 13. Gerhauser C. Cancer cell metabolism, epigenetics and the potential influence of dietary components - a perspective. *Biomed. Res.*, 2012, 1-28.
 14. Pavese JM, Krishna SN, Bergan RC. Genistein inhibits human prostate cancer cell detachment, invasion, and metastasis. *Am. J. Clin. Nutr.*, 2014, 431S-436S.
 15. Ko YH, Smith BL, Wang Y, Pomper MG, Rini DA, Torbenson MS, Hullihen J, Pedersen PL. Advanced cancers: eradication in all cases using 3-bromopyruvate therapy to deplete ATP. *Biochem Biophys Res Commun*, 2004, 269-275.



Oxa-bridged Donor-Acceptor systems containing Triazine core for Dye Sensitized Solar Cell Application

Suma Chemban Subramanian, Maheshkumar Madathikudy Velayudhan,
Manoj Narayanapillai*

Department of Applied Chemistry, Cochin University of Science & Technology, Kochi-22, Kerala, India
(*E-mail: manoj.n@cusat.ac.in)

Abstract: Novel Donor-Acceptor systems of D- π -A-A type incorporating electron deficient triazine moiety as a non-conjugating π -spacer/acceptor with rhodanine acetic acid (DTOP-RHA), barbituric acid (DTOP-BA) or thiobarbituric acid (DTOP-TBA) as anchoring acceptor groups have been synthesized. Diphenylamine is used as the donor moiety and the role of the anchoring group and the π spacer are studied. These dyes are tested as sensitizers in the dye sensitized solar cells. The efficiencies obtained were low compared to the standard dye N719 under identical experimental conditions. This is attributed to the short wavelength absorption characteristics of the dyes as well as the larger energy gap between the LUMO of the dyes and the TiO₂ conduction band.

Key Words: - TiO₂, 1,3,5-Triazine, Donor-Acceptor systems, Electron transfer, DSSC.

INTRODUCTION

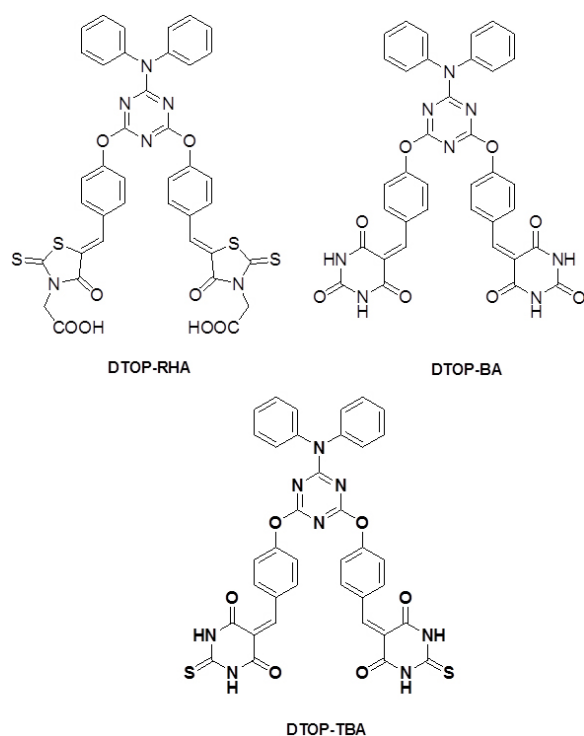
Among emerging photovoltaic device technology, DSSCs and Perovskite cells find an important place. Regarding the efficiencies of these types of cells DSSC report a highest efficiency of 11.9 % and Perovskite cells report 22.1% [1-2]. In recent years, dye-sensitized solar cells (DSSCs) have engrossed much interest due to their potential advantages like cost effective, flexible and straight forward device fabrication [3-9]. Dye sensitized solar cells based on coordination complexes with heavy metal ions are considered as the most efficient device, but cannot be used for large scale applications due to the limited resources and high cost [10-13]. The challenge is open to develop new systems using cost effective materials and promising photoconversion efficiencies. Use of organic D- π -A dyes are one such option with promising results. Most widely studied D- π -A systems include triphenylamine as the donor and cyanoacrylic acid moiety as acceptor [14-17]. Different π spacers with planar configuration, effectively improve the electron-transportation from donors to acceptors and results in significant change in overall photovoltaic performances

[18-20]. Electron deficient heterocyclic structural units such as thiazole, triazine, cyanovinyl, cyano- and fluoro-substituted phenyl groups etc., have been used as the π bridges in the D- π -A-A systems. They exhibit several advantages over the straight D- π -A systems, with significantly changes the molecular energy levels, absorption characteristics and finally the overall photovoltaic performance [21, 22]. 1,3,5-triazine have been used as a building block for the synthesis of D- π -A-A systems as dyes in DSSC. In recent literature triphenylamine or porphyrins have been used in a similar solar cell design with cyanoacrylic acid as the acceptor as well as the anchoring groups. Here we report a series of dyes where diphenylamine as the donor unit and rhodanine acetic acid, barbituric acid or thiobarbituric acid linked to 1,3,5-triazine as the π - acceptor unit.

In simple valence bond terms, when there are two substituents on a benzene ring which are *meta* to each other the possibility of conjugation of π orbitals of one with the other is not possible due to the absence of resonance form of the benzene ring supporting such conjugation. This gives us the possibility of designing dyes having intramolecular charge transfer states, in which Donor and Acceptor moieties are separated in space and thus increase

the length of the charge separation in comparison to directly coupled systems. But such charge separation is useful only when the lifetime of such intramolecular charge separated state is long enough to permit subsequent electron transfer cascade when they are used as dyes and light harvesting systems in photo-voltaic or photo-electrochemical systems. The lifetime of the ICT state depends on the free energy of the back electron transfer regenerating the ground state [23, 24].

Keeping these ideas in mind we have designed dye molecules of D- π -A-A type triads with 1,3,5-triazine as the first acceptor and as the core bridging π unit. Donor moiety chosen was diphenylamine. Rhodanine acetic acid, barbituric acid and thiobarbituric acid were chosen as the second acceptors with varying electron affinity and binding ability to TiO₂ surface. In the current paper we report the synthesis, photophysical and photoelectrochemical properties of these three D- π -A-A type triads. (Scheme1).



Scheme 1. Structures of the compounds

EXPERIMENTAL SECTION

General Techniques

All reagents were obtained from Sigma-Aldrich or Spectrochem at the highest purity and used without further purification. All reactions were carried out at anhydrous conditions and under air/nitrogen

atmosphere. Dimethyl formamide (DMF) and dichloromethane were distilled and dried over molecular sieves (3 Å X 1.5 mm). The ¹H and ¹³C NMR spectra were recorded at 400 MHz Bruker Avance III FT-NMR spectrometer in CDCl₃ or DMSO-d₆. Elemental analysis was performed using Elementar Systeme (Vario EL III) CHN analyser. Molecular mass was determined by electron impact (EI) method on GC-MS (Agilent GC-7890A, Mass-5975C) or ESI on Waters Model e 2695 ESI MS. UV-Vis absorption spectrometry of the dyes in dry DMF solutions were carried out on Thermo Evolution Model 201. All melting points were uncorrected and determined on a Neolab melting point apparatus. FT-IR spectra were recorded using Jasco Model 4100 FT-IR spectrometer. The materials used for DSSC fabrication such as the conducting fluorine Indium Tin Oxide plates (7 Ω/sq), Platisol T, N719 dye, Iodolyte HI-30 and naocrystalline Titania Paste (Ti-Nanoxide) were purchased from Solaronix. Separation and purification of compounds were done by column chromatography using either silica gel (Spectrochem, 60-120 mesh) or neutral alumina (Spectrochem).

Synthesis and Characterization.

Synthesis of 4,6-dichloro-N,N-diphenyl-1,3,5-triazin-2-amine (3)

A solution of cyanuric chloride (100 mmol) in acetone (10 mL) was added slowly to an aqueous solution of NaHCO₃ (100 mmol) at -10 °C followed by diphenylamine (100 mmol) in acetone (10 mL) and stirred for 2 h. The white precipitate obtained was filtered and washed with cold water to remove unreacted cyanuric chloride and dried in vacuum. Column chromatography of the dried precipitate over silica gel using hexane and ethyl acetate (4:1) and drying under vacuum gave colorless crystals of **3** in 63% yield. mp 145 °C. IR (cm⁻¹): 3049, 1489, 1333, 1240. ¹H NMR (400 MHz, CDCl₃ δ ppm): 7.42-7.38 (m, 2H), 7.33-7.28 (m, 1H), 7.27-7.24 (m, 2H). ¹³C NMR (100 MHz, CDCl₃, δ ppm): 170, 165, 141, 129, 127, 124. ESI (m/z): 316.2 (M-1) Anal. Calcd. for C₁₅H₁₀Cl₂N₄ (Mw = 316. 17) C, 56.80; H, 3.18; Cl, 22.36; N, 17.66; found: C, 56.70; H, 3.10; Cl, 22.30; N, 17.60.

4,4'-(6-(diphenylamino)-1,3,5-triazine-2,4-diyl)bis(oxy)dibenzaldehyde (4)

A solution of 4-hydroxybenzaldehyde (20 mmol) in 10 mL of dichloromethane was treated with aqueous NaOH

(50 mL, 0.85 M) at room temperature followed by a solution of compound **3** (100 mmol) in dichloromethane (50 mL) and tetrabutylammonium bromide (TBAB) (20 mol %) was added slowly during 30 minutes. The mixture was stirred for 24 hours and the organic layer was separated and washed well with 10% NaOH, followed by distilled water. The resulting solution was dried with anhydrous Na₂SO₄ and the solvent was removed under vacuum and recrystallization from ethyl acetate to yield **4** as a colourless solid (Yield 63%). mp. 169 °C. IR(cm⁻¹): 1697, 1582, 1375, 1261. ¹H NMR (400 MHz, CDCl₃, δ ppm): 9.95(s, 1H), 7.80-7.77 (d, 2H), 7.28-7.24(m, 4H), 7.19-7.16 (m, 3H). ¹³C NMR (100 MHz, CDCl₃, δ ppm): 190, 171, 167, 156, 142, 133, 130, 129, 127, 126. ESI (m/z): 487.17(M-1), Anal. Calcd. for C₂₉H₂₀N₄O₄ (Mw =488.49) C, 71.30; H, 4.13; N, 11.47, Found: C, 71.20; H, 4.10; N, 11.37.

Synthesis of **5**

General procedure:- A mixture of aldehyde **4** (1 mmol) and of rhodanine-3-acetic acid/barbituric acid/thiobarbituric acid (22 mmol) and ammonium acetate (19 mmol) were dissolved in 0.5 M glacial acetic acid and heated at 120 °C for 12 h. After cooling, the precipitated target product was washed with chloroform and methanol to remove the unreacted reagents and starting materials.

DTOP-RHA (**5a**) Yellow powder. Yield 58%. IR(cm⁻¹): 3330, 1707, 1598, 1501, 1323, 1289. ¹H NMR (400 MHz, DMSO, δ ppm): 7.81 (s, 1H), 7.62-7.60 (d, 2H), 7.38-7.31 (m, 6H), 7.22 (m, 2H), 4.58 (s, 2H). ¹³C NMR (100 MHz, DMSO, δ ppm): 185, 171, 131, 128, 127, 122. Anal. Calcd for C₃₉H₂₆N₆O₈S₄ (Mw= 834.92). C, 56.10; H, 3.14; N, 10.07; S, 15.36; found: C, 56.05; H, 3.10; N, 9.97; S, 15.30.

DTOP-BA (**5b**) Yellow powder. Yield 68%. IR(cm⁻¹): 3325, 1603, 1390, 1115. ¹H NMR (400 MHz, DMSO, δ ppm): 11.23 (s, 1H), 11.10 (s, 1H), 10.79 (s, 1H), 8.30-8.21 (m, 4H), 7.31-6.88 (m, 5H). ¹³C NMR (100 MHz, DMSO, δ ppm): 163.0, 153.1, 150.1, 136.5, 132.6, 129.1, 127.7, 127.4. Anal. Calcd. for C₃₇H₂₄N₈O₈ (MW =740.77). C, 62.71; H, 3.41; N, 15.81; Found C, 62.65; H, 3.31; N, 15.75.

DTOP-TBA (**5c**) Yellow powder. Yield 66%. IR(cm⁻¹): 3460, 1655, 1546, 1364, 1209, 1152. ¹H NMR (400 MHz, DMSO, δ ppm): 12.36 (s, 1H), 12.25 (s, 1H), 8.16 (s, 1H), 8.13-8.11 (d, 2H) 7.29-7.22 (m, 6 H), 7.14-7.10 (m, 1H). ¹³C NMR (100 MHz, DMSO, δ ppm): 178, 170, 159, 154, 142, 135, 130, 128, 127, 122, 121, 118. Anal. Calcd. for C₃₇H₂₄N₈O₆S₂ (MW =708.64) C, 59.99; H, 3.27; N, 15.13; S, 8.66; found: C, 59.89; H, 3.20; N, 15.05; S, 8.60.

Electrochemical measurements

The electrochemical properties of the dyes were investigated by cyclic voltammetry (CV) and square wave voltammetry on a BAS 50W electrochemical workstation using a three electrode configuration. A glassy carbon electrode was used as the working electrode, platinum wire was used as the counter electrode and reference electrode used was Ag/AgCl. A 0.1 M DMF solution of *n*-Bu₄NPF₆ was used as the electrolyte. The solutions were saturated with argon prior to measurements. Ferrocene was used as a reference to standardize the measurements and the corrected values are reported against standard hydrogen electrode (SHE).

DSSC Fabrication and Characterization

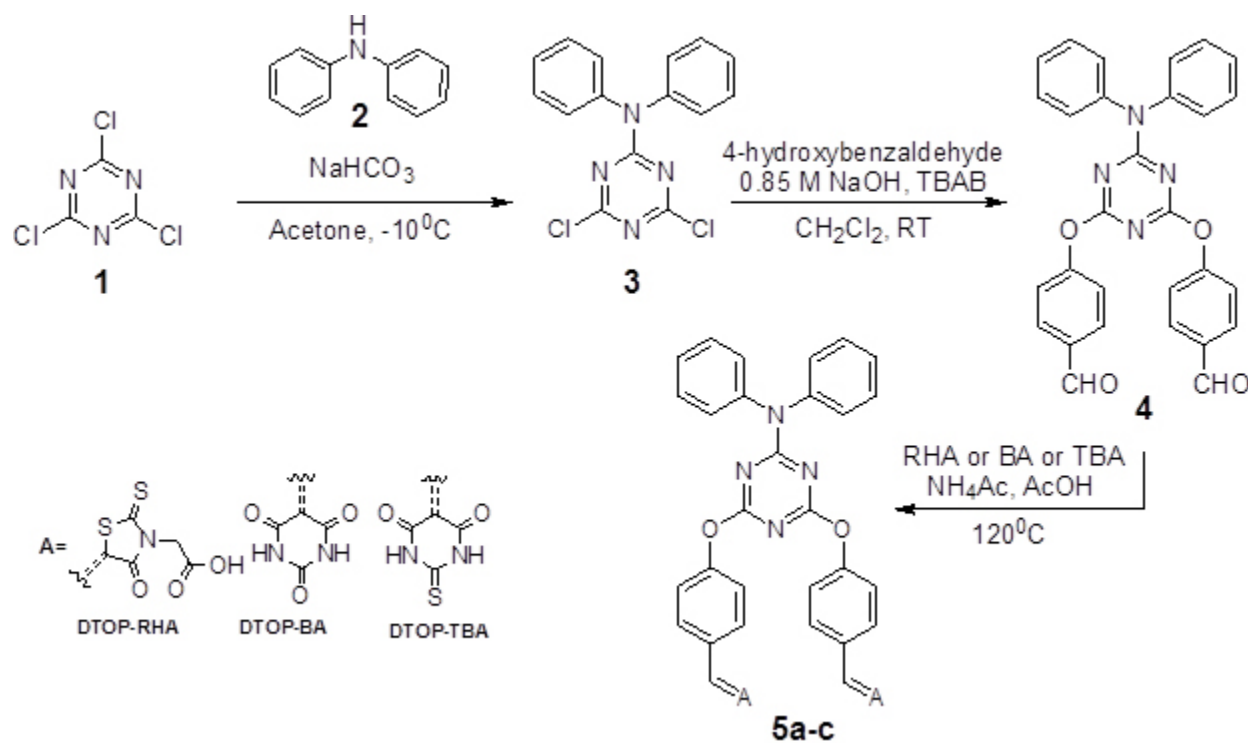
The photoelectrochemical properties of these dyes were studied by constructing photoelectrochemical cells using dye adsorbed TiO₂ as the photoanode, Pt coated Fluorine doped ITO as the cathode and I⁻/I₃⁻ containing LiI 0.4 M and 0.04 M I₂ in dried CH₃CN solution or Br⁻/Br₃⁻ LiBr 0.4 M, 0.04 M Br₂ in dry CH₃CN is used as the redox electrolyte. The preparation of the photoelectrodes and the fabrication of the DSSCs were carried out based on earlier reported methods [25]. The TiO₂ thin films were dipped in dye solution in DMF for 24 hours and washed successively with DMF, water and ethanol. Prior to measurements the cells were dried under vacuum in vacuum desiccators at room temperature. Dark and illuminated I-V characteristics of the cell were measured using a Keithley (2420C) Source Measure Unit. The cell was illuminated using a photo emission tech solar simulator. The photoanode was prepared by coating TiO₂ paste in a rectangular shape on the surface of FTO glass plate by doctor blade method followed by calcination at 450°C for 30 minutes. The TiO₂ electrodes were soaked in dye solution overnight and washed several times with DMF followed by methanol and dried. Pt coated FTO having drilled holes (1mm) for injecting appropriate electrolyte was used as the cathode. The dye coated electrode and the Pt counter electrode were assembled in a sealed sandwich model cell using meltonix as the binder. The active area of the cell was 0.16 cm² and the remaining area was masked with a black tape prior to characterization.

RESULTS & DISCUSSION

Design and Synthesis

We have made use of the ability of cyanuric chloride to undergo nucleophilic substitution reactions with amines and alcohols. All the chlorine atoms of cyanuric chloride can be substituted by primary amines or alcohols at room temperature or at slightly elevated temperatures. However, mono-substitution by nucleophiles requires low temperatures and in the present synthesis mono-substitution by diphenylamine was ensured by carrying

out the reaction at $-10\text{ }^{\circ}\text{C}$ using NaHCO_3 as a base. The remaining chlorine atoms were substituted successfully at room temperature by the *in situ* generated phenoxide anion of 4-hydroxybenzaldehyde with 10% NaOH in dichloromethane in the presence of a phase transfer catalyst tetrabutylammonium bromide. The dialdehyde was made to react with two equivalents of rhodanine acetic acid, barbituric acid or thiobarbituric acid to produce the corresponding D- π -A type triads. All these were soluble in DMF and DMSO. Moderate solubility was observed in methanol and in acetonitrile. DMF was used as the solvent for photophysical as well as electrochemical studies.



Scheme 2. Synthetic Route for the dyes 5a-c

Photophysical studies

Absorption spectra of all dyes show characteristic charge transfer absorption bands around 370 nm , with onset of absorption extending to 450 nm (dark line in Figure 1a-c). The diffuse reflectance spectra of all the compounds in the powder form however show broad absorption spectra peaking at 400 nm and the onset of absorption extending to 500 nm (cf. supplementary data). This red shift could be due to the stacking arrangement that facilitate intramolecular charge transfer [26].

The ability of these dyes in binding with TiO_2 was probed by adding colloidal TiO_2 prepared in aqueous acetic acid medium to the dye solution in DMF. The absorption spectra of DTOP-RHA and DTOP-BA did not show any change upon addition of colloidal TiO_2 . However, DTOP-TBA showed a decrease in the absorbance at 372 nm . This could be due to protonation of the oxa- bridge followed by nucleophilic displacement of the acceptor unit by hydroxyl anions in the colloidal TiO_2 solution. Nano-crystalline TiO_2 thin films were made from a paste of TiO_2 by doctor blading and annealing at $500\text{ }^{\circ}\text{C}$

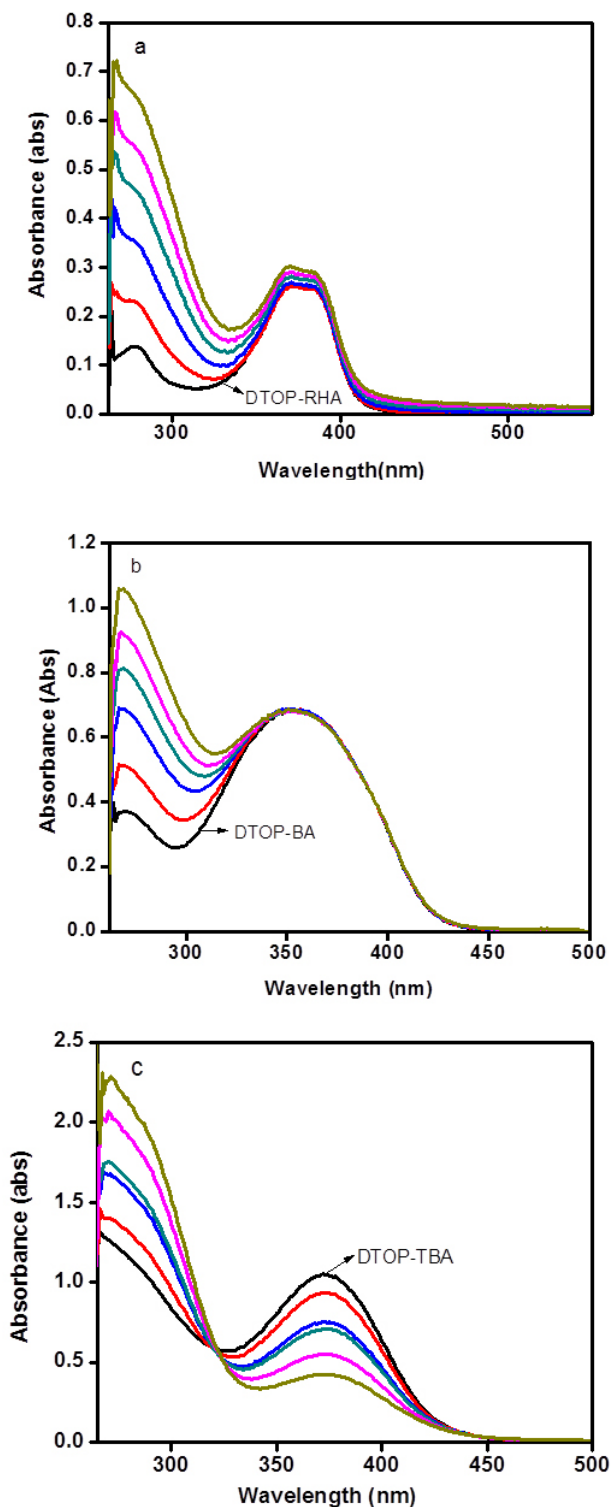


Fig 1. Comparison of the UV-Visible absorption spectrum of dyes a) DTOP-RHA, b) DTOP-BA, c) DTOP-TBA in DMF solution (dark line) and in the presence of increasing amounts of colloidal TiO₂ (10 – 300 μM).

for 30 minutes in a muffle furnace and dye coated TiO₂ thin films were prepared immersing these thin films in respective dye solutions in DMF for 24 h. All films showed light yellow color and attempts to get diffuse reflectance spectra were not successful due to high reflectance of the thin films. Figure 1 shows a comparison of the absorption spectrum of the dyes in DMF solution and the spectrum obtained at different concentrations of colloidal TiO₂. In order to determine the singlet excited state energy of these dyes fluorescence emission spectra were obtained by exciting the dye solutions in DMF at 370 nm (Figure 2). The singlet excitation energy E_{0-0} was calculated from the point of intersection of the normalized absorption and emission spectra of each dye. Photophysical properties of all the dyes were summarized in Table 1.

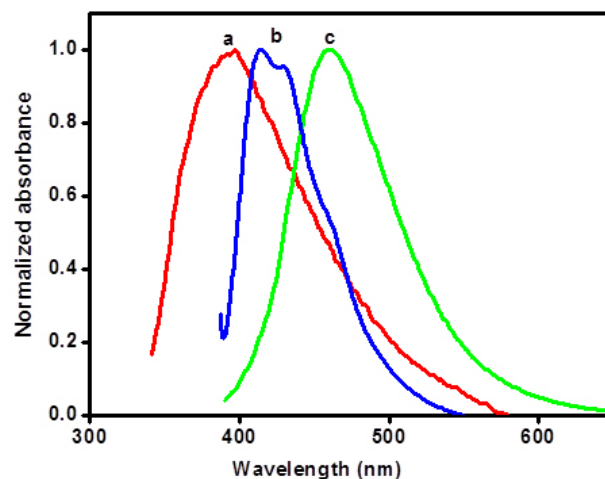


Fig 2. Fluorescence spectra of compounds DTOP-BA (a), DTOP-TBA (b) and DTOP-RHA (c) in DMF ($\sim 1 \times 10^{-8}$ M, $\lambda_{ex} = 370$ nm).

Electrochemical Properties

The oxidation potentials of these dyes were determined from the square wave voltammograms (cf. supplementary data) of these dyes. They exhibit characteristic oxidation potentials at 1.26, 1.26 and 1.22 V respectively vs. NHE [27]. The results are summarized in Table 2. These values are lower than the redox potential of redox couples I⁻/I₃⁻ and Br⁻/Br₃⁻ the common redox couples used in the construction of DSSC's. The energy gap between the redox couple and oxidation potential of the dye is significant in determining the current as well as the fill factor. For the dyes used in the present study the energy gap obtained is very large for I⁻/I₃⁻ (0.53 vs NHE) is 0.73 V in comparison

to Br⁻/Br₃⁻ (1.09 V vs NHE) which is 0.17 V which makes the regeneration of the oxidized dye thermodynamically favorable during the operation of the cell [28]. The HOMO and the LUMO energies of these dyes referenced to NHE were calculated from the oxidation potentials of these dyes

and their respective singlet energy. Estimations of HOMO and LUMO energies against vacuum continuum were also been made and all the values are presented in Table 2 [29-30].

Table 1. Photophysical properties of DTOP-RHA, DTOP-BA and DTOP-TBA in DMF.

Dyes	λ_{\max} (Abs) nm	ϵ_{\max} dm ³ mol ⁻¹ cm ⁻¹	λ_{\max} (Em) nm	$E_{0,0}$ eV	E_{ox} V vs. SHE
DTOP-RHA	370 390*	2.55 × 10 ³	430	3.04	1.26
DTOP-BA	373 375*	2.18 × 10 ³	405	3.1	1.26
DTOP-TBA	375 380*	2.3 × 10 ³	405, 429	3.06	1.22

Table 2. Electrochemical properties and band gaps of DTOP-RHA, DTOP-BA and DTOP-TBA in DMF.

Dyes	$E_{on set}$ in DMF	$E_{onset (ox)}$ Vs E_{FOC}/V	$E(S+/S)$ vs NHE/ V	E_{0-0} (eV)	LUMO vs NHE/eV	E_{gap}/V	HOMO(IP)/eV	LUMO (EA)/eV
DTOP-RHA	1.17	1.06	1.26	3.04	-1.78	1.28	-6.06	-2.98
DTOP-BA	1.17	1.06	1.26	3.1	-1.84	1.34	-6.06	-2.96
DTOP-TBA	1.13	1.02	1.22	3.04	-1.82	1.32	-6.02	-2.98

$E_{FOC} = -0.11$ V vs. Ag/AgCl the ground-state oxidation potentials $E(S+/S)$ (HOMO) were measured in DMF containing 0.1 M tetrabutylammonium hexafluorophosphate as supporting electrolyte using a glassy carbon working electrode, a Pt counter electrode and a Ag/AgCl reference electrode; the E_{0-0} value was estimated from the cross-section of absorption and emission spectra; E_{gap} is the energy gap between LUMO of the dye and the conduction band level of TiO₂ (-0.5 V vs. NHE); ionization potential: IP = - 4.8 - ($E_{onset (ox)} - E_{FOC}$); electron affinity: EA - E_{0-0} = IP

Theoretical Study

The optimized geometry of the dyes as well as the frontier orbitals and their energies are computed by density functional theory (DFT) with B3LYP exchange-correlation functional [31, 32] and 6-31+G(d) basis set. The stationary points are characterized by frequency calculation. To include the effects of solvation the polarization continuum model (PCM) for DMF has been used in the calculations. All calculations were performed with the GAUSSIAN09 quantum chemistry package. The calculations were repeated with B3P86 functional and

found no significant variation in the geometry and orbital energies obtained by B3LYP functional correlated well with the experimental data (Table 3). The optimized geometry along with the frontier orbital representation and their respective energies against vacuum continuum is given in Figures 3. Contrary to our expectation the orbital coefficients of the HOMO for all compounds were found to be delocalized over the triazine core which is one of the acceptor units. This delocalization extends over the terminal rhodanine-3-acetic acid acceptor unit in the case of the dye DTOP-RHA. Delocalization of HOMO over the triazine has a profound effect in the lowering of HOMO energies as well as on the observed oxidation potential of all the dyes. Both electrochemical and theoretical data suggests that they are difficult to oxidize in comparison to oxidation of diphenylamine. This also explains the higher excitation energy and thus lower coverage of the solar spectrum in the visible region. The dyes DTOP-BA and DTOP-TBA show better directionality of charge transfer as the HOMO and LUMO are localized on different regions of the molecule. This effect is evident in the more red shifted absorption spectrum obtained for these dyes. The theoretically calculated energy levels are also found to be matching with the experimental values obtained from

electrochemical measurements. The utility of these dyes in the fabrication of DSSCs was assessed by comparing the redox levels of the dyes, redox electrolytes and the TiO₂ photoanode. Figure 4 illustrates this comparison and it is

evident that the electron injection by the excited dye to the TiO₂ photoanode and the regeneration of the dye by the redox electrolyte are exergonic.

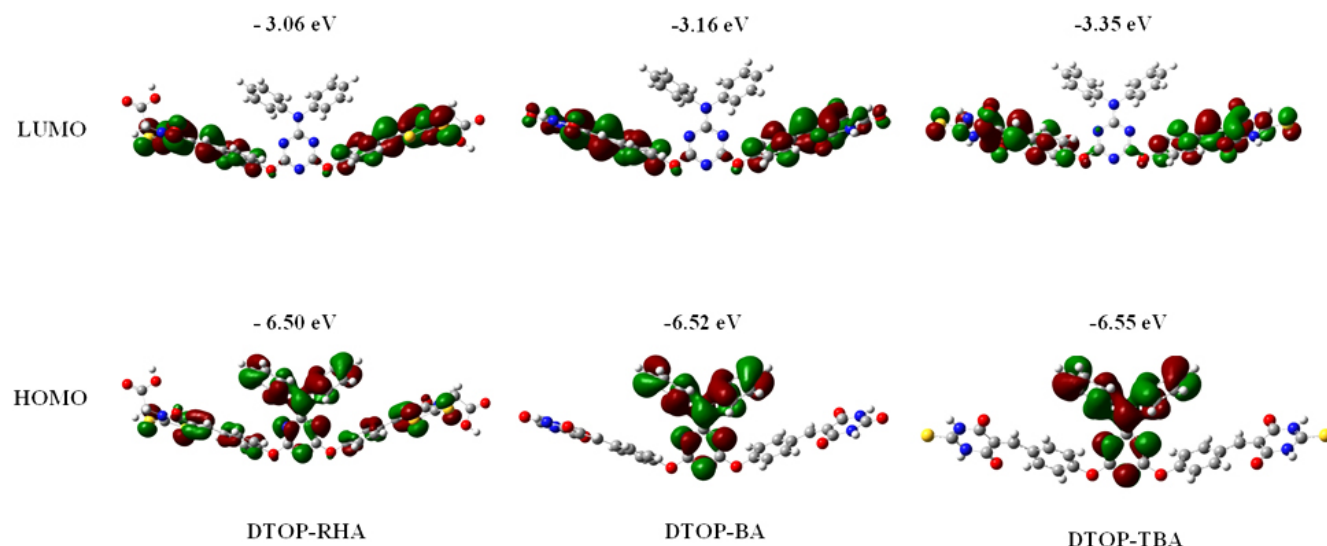


Fig 3. Optimized geometries of the dyes computed using DFT theory at the B3LYP/6-31G level

Table 3. Comparison of theoretically and experimentally determined energies of HOMO and LUMO orbitals of dyes DTOP-RHA, DTOP-BA and DTOP-TBA. (Values in parenthesis are those obtained for B3P86 functional.)

Dyes	Experimental		Theoretical (DFT-B3LYP)	
	HOMO (V)	LUMO(V)	HOMO (V)	LUMO (V)
DTOP-RHA	-6.64	-3.05	-6.50 (-7.15)	-3.06, (-3.70)
DTOP-BA	-6.63	-3.53	-6.52 (-7.16)	-3.16 (-3.80)
DTOP-TBA	-6.50	-3.64	-6.55 (-7.20)	-3.35 (-3.99)

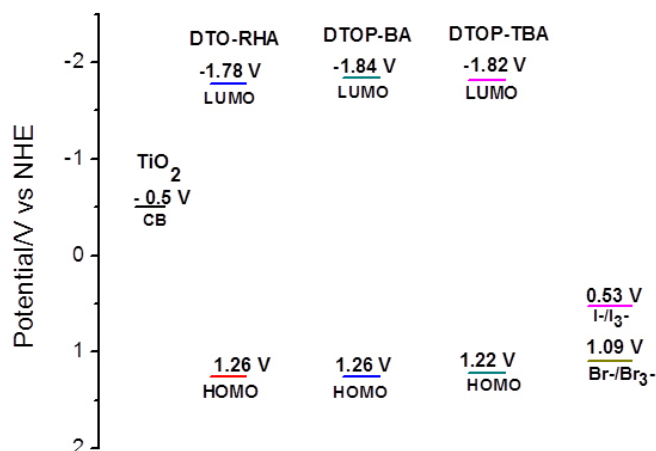


Fig 4. Schematic energy level diagram for a DSSC based on dyes attached to nanocrystalline TiO₂ film deposited on conducting FTO.

Photoelectrochemical Properties

Under illumination by a 1.5 AM light source all the cells constructed gave I-V characteristics for typical photodiodes. A few representative J-V curves obtained for dyes DTOP-RHA, DTOP-BA and DTOP-TBA when Br⁻/Br₃⁻ was used as the electrolyte are given in Figure 5. The solar cell parameters obtained from the photocurrent measurements were summarized in Table 4. The solar energy to electrical energy conversion efficiency was calculated from Open circuit voltage, short-circuited current, fill factor and the incident photon flux (P_{in}) by using equation,

$$\eta = \frac{J_{sc} V_{oc} FF}{P_{in}} \quad (\text{Eq. 1})$$

Under our experimental conditions an efficiency of 3 % was obtained for the N719 dye when I⁻/I₃⁻ was used as the electrolyte. The results show that the observed conversion efficiency are lower and are in the range of 0.01 – 0.06 where the cell made from the dye DTOP-TBA with Br⁻/Br₃⁻ was found to be the most efficient in the series. The data obtained for the cells with I⁻/I₃⁻ as the electrolyte were very low in comparison to the data obtained for Br⁻/Br₃⁻ in terms of Voc and thus η. This could be due to the low potential difference between the Fermi level and the high lying redox potential of I⁻/I₃⁻ in comparison to Br⁻/Br₃⁻. The poor efficiency data observed could be due to a combined effect of lower coverage of the solar spectrum by the dyes as well as lower binding coefficients. Relatively better performance of DTOP-TBA may be the result of the high lying HOMO making regeneration of the dye efficient in comparison to other dyes. Based on a similar design strategy better performing dye sensitizers can be synthesized by incorporating better donor groups and by incorporating groups that enhance conjugation at the acceptor site.

Table 4. DSSC Performance data of the dyes

Dyes	J _{sc} , mA cm ⁻²	V _{oc} , mV	FF, %	η, %
DTOP-RHA	-0.160 ^a (0.001)	0.273 ^a (0.001)	45 ^a (3.78)	0.02 ^a (0.002)
	-0.078 ^b (0.006)	0.477 ^b (0.007)	79 ^b (6.65)	0.03 ^b (0.0007)
DTOP-BA	-0.094 ^a (0.001)	0.210 ^a (0.002)	50 ^a (1.5)	0.01 ^a (0.0004)
	-0.124 ^b (0.005)	0.580 ^b (0.004)	62 ^b (2.0)	0.04 ^b (0.0005)
DTOP-TBA	-0.129 ^a (0.005)	0.182 ^a (0.008)	42 ^a (5.29)	0.01 ^a (0.0005)
	-0.215 ^b (0.00)	0.475 ^b (0.004)	58 ^b (3.5)	0.06 ^b (0.0004)

a* I⁻/I₃⁻ electrolyte. b* Br⁻/Br₃⁻ electrolyte

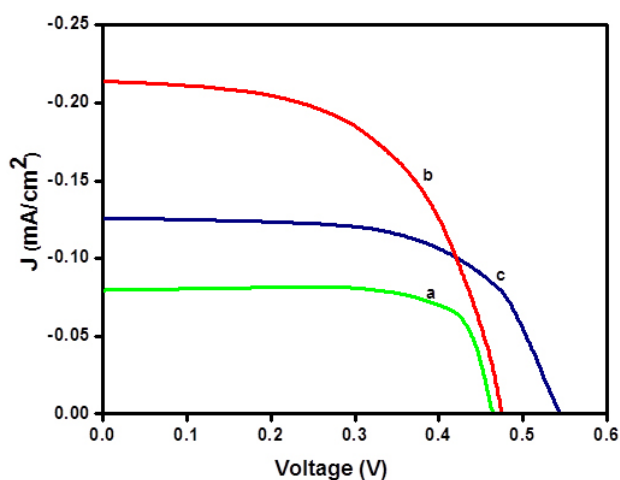


Fig 5. Photocurrent density–voltage curves of the compounds DTP-RHA (a), DTP-BA (b) and DTP-TBA (c) using Br⁻/Br₃⁻ electrolyte

CONCLUSION

We have designed and synthesized three novel D-π-A-A systems with triazine core as the non-conjugating spacer/acceptor with rhodanine-3-acetic acid (DTOP-RHA), barbituric acid (DTOP-BA) or thiobarbituric acid (DTOP-TBA) as anchoring acceptor groups. Electrochemical, photophysical studies and theoretical studies show that they have suitable properties for use as dyes in dye sensitized solar cells. The applicability of these dyes for the DSSC was tested by constructing the sandwich model cell. However, the observed efficiency was lower than that obtained for N719 dye under similar experimental conditions. This is attributed to the low coverage of the solar spectrum and large energy gap between the LUMO of the dyes and the conduction band of the TiO₂.

The results suggest tuning of the LUMO energy by incorporating additional conjugating groups in the acceptor side of the design. Further studies in this direction are progressing.

REFERENCES

1. Sarah, K.; Keith E., National Renewable Energy Laboratory (NREL), Golden, CO, February 2016, https://en.wikipedia.org/wiki/Solar_cell
2. Seo, J.; Noh, J. H.; Seok, S. I., *Acc. Chem. Res.* **2016**, *49*, 562–572.
3. Hagfeldt, A.; Graetzel, M., *Chem. Rev.* **1995**, *95*, 49–68.
4. Do, K.; Choi, H.; Lim, K.; Jo, H.; Cho, J. W.; Nazeeruddin, M. K.; Ko, J., *Chem. Commun.* **2014**, *50*, 10971–10974.
5. Liu, J.; Wang, K.; Zhang, X.; Li, C.; You, X., *Tetrahedron.* **2013**, *69*, 190–200.
6. Ning, Z.; Tian, H., *Chem. Commun.* **2009**, 5483–5495.
7. Ooyama, Y.; Harima, Y., *Eu. J. Org. Chem.* **2009**, 2903–2934.
8. Sharma, G. D.; Angaridis, P. A.; Pipou, S.; Zervaki, G. E.; Nikolaou, V.; Misra, R.; Coutsolelos, A. G., *Org. Electron.* **2015**, *25*, 295–307.
9. Zervaki, G. E.; Roy, M. S.; Panda, M. K.; Angaridis, P. A.; Chrissos, E.; Sharma, G. D.; Coutsolelos, A. G., *Inorg. Chem.* **2013**, *52*, 9813–9825
10. Bella, F.; Gerbaldi, C.; Barolo, C.; Gratzel, M., *Chem. Soc. Rev.* **2015**, *44*, 3431–3473.
11. Grätzel, M., *Nature.* **2001**, *414*, 338–344.
12. Nazeeruddin, M. K.; Pechy, P.; Renouard, T.; Zakeeruddin, S. M.; Humphry-Baker, R.; Comte, P.; Liska, P.; Cevey, L.; Costa, E.; Shklover, V.; Spiccia, L.; Deacon, G. B.; Bignozzi, C. A.; Gratzel, M., *J. Am. Chem. Soc.* **2001**, *123*, 1613–1624.
13. Nazeeruddin, M. K.; Zakeeruddin, S. M.; Humphry-Baker, R.; Jirousek, M.; Liska, P.; Vlachopoulos, N.; Shklover, V.; Fischer, C. H.; Gratzel, M., *Inorg. Chem.* **1999**, *38*, 6298–6305.
14. Hwang, S.; Lee, J. H.; Park, C.; Lee, H.; Kim, C.; Park, C.; Lee, M.-H.; Lee, W.; Park, J.; Kim, K.; Park, N.-G.; Kim, C., *Chem. Commun.* **2007**, 4887–4889.
15. Xu, M.; Li, R.; Pootrakulchote, N.; Shi, D.; Guo, J.; Yi, Z.; Zakeeruddin, S. M.; Graetzel, M.; Wang, P., *J. Phys. Chem. C.* **2008**, *112*, 19770–19776.
16. Sayama, K.; Hara, K.; Mori, N.; Satsuki, M.; Suga, S.; Tsukagoshi, S.; Abe, Y.; Sugihara, H.; Arakawa, H., *Chem. Commun.* **2000**, 1173–1174.
17. Hara, K.; Sayama, K.; Ohga, Y.; Shinpo, A.; Suga, S.; Arakawa, H., *Chem. Commun.* **2001**, 569–570.
18. Horiuchi, T.; Miura, H.; Sumioka, K.; Uchida, S., *J. Am. Chem. Soc.* **2004**, *126*, 12218–12219.
19. Wang, Z.-S.; Koumura, N.; Cui, Y.; Takahashi, M.; Sekiguchi, H.; Mori, A.; Kubo, T.; Furube, A.; Hara, K., *Chem. Mater.* **2008**, *20*, 3993–4003.
20. Song, J.-L.; Amaladass, P.; Wen, S.-H.; Pasunooti, K. K.; Li, A.; Yu, Y.-L.; Wang, X.; Deng, W.-Q.; Liu, X.-W., *New J. Chem.* **2011**, *35*, 127.
21. Wu, Y.; Zhu, W., *Chem. Soc. Rev.* **2013**, *42*, 2039–2058.
22. Zhong, H.; Xu, E.; Zeng, D.; Du, J.; Sun, J.; Ren, S.; Jiang, B.; Fang, Q., *Org. Lett.* **2008**, *10*, 709–712.
23. Suneesh, C. V.; Vinayak, M. V.; Gopidas, K. R., *J. Phys. Chem. C.* **2010**, *114*, 18736–18744.
24. Suneesh, C. V.; Gopidas, K. R., *J. Phys. Chem. C.* **2010**, *114*, 18725–18734.
25. Zervaki, G. E.; Roy, M. S.; Panda, M. K.; Angaridis, P. A.; Chrissos, E.; Sharma, G. D.; Coutsolelos, A. G. *Inorg. Chem.* **2013**, *52*, 9813–9825.
26. Zhong, H.; Lai, H.; Fang, Q., *J. Phys. Chem. C.* **2011**, *115*, 2423–2427.
27. Neil, G.; William, E. G., *Chem. Rev.* **1996**, *96*, 877–910.
28. Wang, Z. S.; Sayama, K.; Sugihara, H., *J. Phys. Chem. B.* **2005**, *109*, 22449–22455.
29. Xie, Q. J.; Kuwabata, S.; Yoneyama, H., *J. Electroanal. Chem.* **1997**, *420*, 219–225.
30. Fermin, D. J.; Teuel, H.; Scharaifker, B. R., *J. Electroanal. Chem.* **1996**, *401*, 207–214.
31. Lee, C.; Yang, W.; Parr, R. G., *Phys. Rev. B.* **1988**, *37*, 785–789.
32. Becke, A. D., *J. Chem. Phys.* **1993**, *98*, 5648–5652.

The Need for Nanometry Education

David Devraj Kumar

STEM Education Laboratory, College of Education, Florida Atlantic University, Davie, FL 33314
(*E-mail: david@fau.edu)

Abstract: The need for nanometry education is presented. As operationally defined, nanometry education is the “art, science and process of teaching and learning nanoscale measurements” [1, p. 59]. Using instructional activities based on carefully identified benchmark characteristics of objects, it is possible to cultivate an understanding in students of the scale of a wide range of seen and unseen objects tapping into the power of children’s imagination and inference skills. Since high teacher quality is the key to successful children’s education, it is essential that nanometry education be part of teacher preparation curricula in the science, technology, engineering and mathematics (STEM) education.

Key Words: Need, Nanometry Education, Nanoscale, Teaching, Learning

INTRODUCTION

Nanometry education is the creative art of illustrating, the science of exploring, and the process of understanding measurements of materials at the nanoscale in teaching and learning [1]. Nanoscale materials continue to impact science and technology in the twenty-first century. The US federal government has invested billions of dollars in research and development efforts in this rapidly growing field, not to mention the many millions of dollars invested in curricular reform efforts in education involving nanoscale materials [2]. However, teaching about matter at the nanoscale at K-12 still remains a challenge since teachers-in-training themselves find it difficult to comprehend this concept [3, 4]. For example, a study of 109 undergraduate science education students reported item difficulty (proportion of students answering correctly) values 0.257 and 0.073 respectively [4] for the following two items [5]: (1) If a nanometer were about as big as the width of a pinhead, about how long would a meter be? (a) as long as the pin shaft, (b) as long as a ladder, (c) as long as a blue whale, (d) as long as a trip between Washington, D.C., and Atlanta, Georgia and (2) How many hydrogen atoms lined up “shoulder to shoulder” would fit in a one nanometer space? (a) less than one, (b) ten, (c) one thousand, (d) one billion.

BENCHMARK CHARACTERISTICS

An understanding of the scale of a wide range of seen and unseen objects is critical because “scale is one of the thematic threads that runs through all of the sciences” [6, p. 409]. Using carefully identified benchmark characteristics of objects may be one way to create a meaningful context for students to visualize the nanoscale in nanometry education. For example, the width of an average house (10m) is 100,000 times larger than that of an average human hair (100 μ m) the diameter of an average human hair is 100,000 larger than that of a single-walled carbon nanotube (1nm) (National Center for Electron Microscopy, n.d.) (Figure 1).



Fig 1. Benchmark characteristics of objects.
(Courtesy of National Center for Electron Microscopy, Berkeley, CA, US Department of Energy, National Nanotechnology Coordination Office.)

Another set of benchmark characteristics of objects is presented in Figure 2, where the scale ranges from 0.1nm (water molecule) to 100,000,000nm (tennis ball). Such illustrations help to form mental pictures of objects invisible to the naked eye and play a significant role in the formation of mental associations during learning. Also, they are useful tools for integrating science at the nanoscale with overlapping mathematical concepts [7].

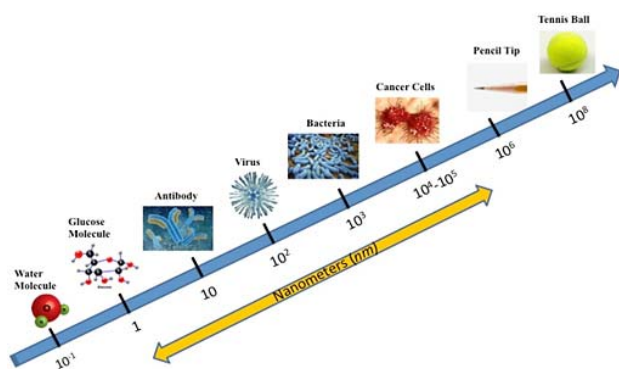


Fig 2. Scale of benchmark characteristics of objects from 10^{-1} nm to 10^8 nm.

FINAL THOUGHTS

It takes a high level of imagination to visualize nanoscale materials and to infer their characteristics in relation to visible objects. Using mathematical relationships that are suitable for understanding the scale conversions may not be easy for those who tend to distance themselves from mathematics. Carefully developed nanometry education activities can help children even as early as at elementary grade levels develop mathematical as well as scientific thinking skills suggested by the National Council of Teachers of Mathematics (NCTM) and National Science Education Standards (NSES). For example, NCTM Grades 3–5 Expectations state all students should “understand the place-value structure of the base-ten number system and be able to represent and compare whole numbers and decimals.” Therefore, it is necessary that realistic, meaningful teaching methods that enable students to visualize and infer the scale of the world of nano materials be developed and implemented in science classrooms.

Teachers-in-training should be given pedagogically relevant opportunities for discussing and developing cognitively engaging ways of teaching nanometry in

science classrooms. In order to fully take advantage of the pedagogical benefits of education involving nanoscale materials and contribute towards STEM workforce development, it is highly important that nanometry education be made an integral part of STEM teaching and learning.

ACKNOWLEDGMENT

Thanks to Chelsea Dittrich and Sylvia Collazo for thoughtful feedback and to Ramzy Baroodi for assistance with the scale of benchmark characteristics of objects.

REFERENCES

1. Kumar, D. D. (2016). Nanometry in science teaching. *School Science Review*, 97(361), 59-62.
2. National Nanotechnology Initiative. (n.d.). *Education*. Nano.gov. Available at: <https://www.nano.gov/education-training>
3. Albe, V. (2011). *Nanoscience and Nanotechnologies Education: Teachers' Knowledge*. Available at: www.esera.org/media/ebook/strand13/ebook-esera2011_ALBE-13.pdf
4. Kumar, D. D. (2007). Nanoscale science and technology in teaching. *Australian Journal of Education in Chemistry*, 68, 20-22.
5. NIST. (n.d.). *Nano IQ*. National Institute of Standards and technology. Available at: nanosense.sri.com/activities/sizematters and www.nist.gov/public_affairs/kids/nanotechquiz.htm
6. Jones, M. G., Tretter, T., Taylor, A., & Oppewal, T. (2008). Experienced and novice teachers' concepts of spatial scale. *International Journal of Science Education*, 30, 409-429.
7. Kumar, D. D., Ridener, B., & Bindu, R. L. (2013). Teaching nanoscale through integrated science and mathematics. In Sinha, M. (ed.), *Redefining education: Expanding horizons*. New Delhi: Alfa Publications.



Public Understanding of Chemistry: Chemistry and its social-political-economic contexts continue to change.

Chemistry and chemistry-based technology that impact our lives make for the complexity and controversy of life and set the stage for thinking about public understanding of chemistry. The Public Understanding of Chemistry section will try to address chemistry in real life context with original contributions (articles/position papers/policy briefs) and/or published articles and columns in reputable sources (used with permission).

Founding Section Editor: David Devraj Kumar, **Section Co-Editor:** David M. Manuta

BUILDING INTERDISCIPLINARY BRIDGES FOR SCIENCE

John Baglin

IBM Almaden Research Center, San Jose, CA 95120

(Email: baglin@us.ibm.com)

Connecting the Disciplines

We are fortunate to live in a world where the bountiful fruits of fast-developing science and technology enrich the lives and accomplishments of most people on the planet – and influence the development of the whole global community. It is increasingly apparent that good research planning and effective application of our new discoveries must rely on responsible and well-informed integration of information and expertise from diverse (yet intrinsically connected or overlapping) fields of science, engineering, and policy.

This situation presents a fine opportunity for our educators to consider innovative and constructive ways to develop both tools and systems that will stimulate and assist interdisciplinary communication among the many fields of science. A key to success will be effective communication between scientists and the institutions of the general community.

It is neither possible nor desirable to contemplate total intermixing of disciplines. Instead, we need to consider building bridges that will facilitate contact and interaction among people who work in diverse fields, and also facilitate their contact with people in the broader community. Such bridge-building is often an unfamiliar art that will demand the best skills of our communities of Education and Policy in order to bring it to full fruition.

The following paragraphs illustrate some types of bridge building that are needed, and some corresponding actions to consider for building those bridges.

Abstract: Our world increasingly depends on new scientific and technical discoveries and inventions. Often, those with highest potential impact for the human condition (such as DNA editing, nanoscale electronic devices, etc.) intrinsically involve interfaces between classical scientific disciplines. Similarly, there is a need to nurture interfaces between scientists and the general community. This 'opinion' essay suggests some areas where we can take constructive steps to promote healthy, well-integrated progress of enterprising research, with optimal implementation, supported by community awareness. Timely action is needed, not only to develop updated formal academic curricula, but also to create attractive options for up-to-date life-long learning.

Key Words: Inter-disciplinary integration, science education; community outreach, scientific literacy.

Interdisciplinary Bridges among the Sciences

In many school programs and institutions, and in research programs and professional journals, the historical separation still prevails between Physics, Math, Biology, Chemistry, Metallurgy, etc. despite a growing focus on STEM education designed to encourage integrated studies in technical topics. Meanwhile, increasingly it becomes clearer that many of the newest and best research discoveries and technologies depend on expert interaction involving two or more of the separate disciplines. One conspicuous example lies in the ongoing spectacular progress of biomolecular science research, medical sciences, and genomics. In this new era, much progress is clearly driven by integration at the boundaries between the separate disciplines, for research, enterprise, expertise, and collaboration.

New discoveries thrive on cross-fertilization of ideas, and on effective communication, involving a wide spectrum of the sciences, and their applications. Cross-disciplinary collaboration is evident today in research journals and patents, and in consumer products, whose invention and rapid progress to market increasingly stem from linkages forged between hitherto formally disconnected fields, such as physics, chemistry, bio-sciences, geo-sciences, environmental sciences, communications, computer science, and many scientific and engineering technologies.

We may note incidentally that the “new” field titled Materials Science & Engineering emerged during the 1970s, based on the widespread recognition by the research and teaching communities that an impressive scope for future innovation and understanding would be well served by formal integration of curricula under this title. A leading advocate and ‘father’ of this novel approach was Professor Rustum Roy, of Pennsylvania State University.

Bridges to Community

We need to develop bridges that serve as positive drivers for well-informed decisions, both private and governmental, in areas such as:

- public motivation,
- sound investment,
- effective public health policy,
- societal well-being,
- support of science research,
- setting and execution of government policy - local, national and global

Such bridges will link with areas such as legislation and societal policy, financial planning and management, economic policy, and also urban planning, disaster /risk mitigation, and environmental topics including sustainable food, water, energy and mineral resources. Communication between scientific and civil communities must focus on mutual comprehension and well-founded trust. Good science must be recognized as an integral (and cost-effective) part of policy-setting - at governmental levels, and also in the communities of industry, engineering, commerce and economics.

International Bridges

Sound scientific information and advice are now needed more than ever in fields of universal global impact - where new and locally important research may be wisely supported, with collaboration between well qualified

national communities and institutions of advanced technology. In view of the pervasive global links of trade and economics and inter-governmental relations among nations, the landscape of scientific knowledge and its dissemination, recognition, application, and effective implementation must also be global. Research collaborations across international borders can be constructive. Already, much of the community of scientific research functions with strong professional international links (as evidenced by the collaborative publications in research journals and the thriving interactions among participants at international technology conferences.) Additionally, there exists scope for respected international science organizations like the International Council for Science (ICSU), and National Academies to conduct more in-depth, highly responsible scholarly studies whose published reports may indicate paths toward future optimal world-wide strategies for global resource management (such as global energy and water policies), and strategic issues for medical, epidemiological, and public health programs that can only be addressed effectively at the international level. It is of the highest importance that such reports include recommendations that leave no doubt about the meaning and reliability of their key scientific conclusions, so as to provide compelling foundations upon which business decisions can be responsibly based.

Integrated Science Education

Evidently, it is no longer acceptable to plan curricula for primary and secondary schools in which physics, chemistry, biology, and mathematics (and critical thinking) are taught as disconnected subjects. As already recognized in many parts of the world, new curricula have been devised that present science as a logically integrated combination of such topics. This approach makes sense to the students, who then perceive readily the relevance and applicability to their own current and future life experiences. This also can enable the introduction to scientific thinking to be made earlier in school curricula. Such integrated programs of study then prepare students for tertiary education programs that are also designed to reveal, and capitalize upon, the underlying links between previously isolated disciplines. In turn, graduates in science, technology, and engineering will then be realistically prepared for positions of competence, responsibility, interdisciplinary collaboration, and perhaps leadership in the increasingly technological world.

Bridges to the Future. Life-long Learning

A conspicuous feature of the technological and scientific landscape in recent years is its accelerating pace of change. This is apparent in all kinds of diverse scientific fields, including electronics, human health, biomolecular science, materials science, computer science (Big Data), renewable energy, forestry, forensic sciences, geological, oceanographic and climate studies. This applies also for the social sciences, economics, and political science. One of the most important personal assets needed to equip an individual to participate responsibly in his/her community is some level of "Science Literacy". How well can he/she comprehend and responsibly manage life in the surrounding physical and perceptual world, without some basic level of science literacy? Furthermore, in order to remain qualified (and interested) in his/her technical-related job, everyone (including teachers and academics) will need to continuously acquire new knowledge and skills, and be aware of current innovations in advancing science and technology. Hopefully, their early training and education will have endowed each person with skills and motivation for continuous self-education. In that case, they will be prepared not only to follow new or emerging technologies, but also to think laterally, in various different disciplines. By innovating, and inventing their own new techniques, or making their own new scientific discoveries, they will thus contribute to the current and future well-being of mankind. This is one place where a diversified background, and multi-disciplinary competence, can propel us into fruitful and creative careers, over many years. Early mastery of the

special art, skills, and tools for life-long learning, and early exposure to multiple inter-related aspects of science (even including esoteric or fundamental topics) can have a major impact on the future – personally for those practitioners, and also for the whole world that benefits from their enterprising discoveries, insights, and outreach.

Challenges for Science Education

The above discussion should not be interpreted as proposing that the ideal future world should be populated by superior beings, each having expertise and in-depth knowledge covering the entire spectrum of science and technology fields and professions. This would indeed be an untenable concept! No, we surely should not expect that every brain surgeon must also be an expert brick-layer, poet, and rocket scientist! Professional and occupational specialization must surely continue to be a basis of our functional fabric! However, it is critical for such specialists to have the skills and tools to support excellent mutual interaction, communication and collaboration. Increasingly, we depend on effective teamwork among specialists in related fields, who can overcome interdisciplinary barriers, comprehend each other's technical (and philosophical) vocabulary, and work together professionally.

How can we best design our education systems and objectives so that they support essential inter-disciplinarily in the modern world, while preserving the important goals of professional excellence and specialist function in the multi-faceted real world?

Within the traditional framework of schooling, a priority for all students and levels must surely be to systematically develop science literacy, while the multi-topic core curriculum is being taught. It is to be hoped that, even when core topics are being studied, the students' interest in interdisciplinary exploration can be sparked.

Promotion of STEM education in traditional school programs is indeed valuable. However, it may not extend into the broadest spectrum of inter-disciplinary topics where bridge-building is most needed – especially those areas linking science with public policy. Future success and function for many people will depend on:

- basic knowledge and skills developed by 'traditional' schooling;
- motivation to sustain awareness of new scientific discoveries and technical achievements;
- life-long use of critical thinking;
- analytical curiosity about the world beyond their immediate environment;
- easy and abundant access to stimulating and constructive resources for learning about new fields.

For whatever purpose - personal satisfaction, career advancement, or even survival - tangible rewards can result from such learning.

Interdisciplinary "bridges" as discussed above need to be devised and built, and made attractive, exciting, and readily available to all. They might take many forms, including on-line tutorials, modular courses, newsletters, conferences, search engines, technical social media, or novel forms of on-line consultation. One often-needed resource would be a well-designed set of lexicons in which the technical terminology that is historically embedded in each of the disciplines is briefly but professionally explained for members of different disciplines, at a level sufficient to constitute a 'language bridge' when needed.

Building 'user-friendly' bridges that actually make interdisciplinary participation compellingly attractive and practically rewarding can surely be one of our biggest educational and organizational accomplishments in the coming years.

The AIC Code of Ethics

Approved by the AIC Board of Directors, April 29, 1983



The profession of chemistry is increasingly important to the progress and the welfare of the community. The Chemist is frequently responsible for decisions affecting the lives and fortunes of others. To protect the public and maintain the honor of the profession, the American Institute of Chemists has established the following rules of conduct. It is the Duty of *The Chemist*:

1. To uphold the law; not to engage in illegal work nor cooperate with anyone so engaged;
2. To avoid associating or being identified with any enterprise of questionable character;
3. To be diligent in exposing and opposing such errors and frauds as *The Chemist's* special knowledge brings to light;
4. To sustain the institute and burdens of the community as a responsible citizen;
5. To work and act in a strict spirit of fairness to employers, clients, contractors, employees, and in a spirit of personal helpfulness and fraternity toward other members of the chemical profession;
6. To use only honorable means of competition for professional employment; to advertise only in a dignified and factual manner; to refrain from unfairly injuring, directly or indirectly, the professional reputation, prospects, or business of a fellow Chemist, or attempting to supplant a fellow chemist already selected for employment; to perform services for a client only at rates that fairly reflect costs of equipment, supplies, and overhead expenses as well as fair personal compensation;
7. To accept employment from more than one employer or client only when there is no conflict of interest; to accept commission or compensation in any form from more than one interested party only with the full knowledge and consent of all parties concerned;
8. To perform all professional work in a manner that merits full confidence and trust; to be conservative in estimates, reports, and testimony, especially if these are related to the promotion of a business enterprise or the protection of the public interest, and to state explicitly any known bias embodied therein; to advise client or employer of the probability of success before undertaking a project;
9. To review the professional work of other chemists, when requested, fairly and in confidence, whether they are:
 - a. subordinates or employees
 - b. authors of proposals for grants or contracts
 - c. authors of technical papers, patents, or other publications
 - d. involved in litigation;
10. To advance the profession by exchanging general information and experience with fellow Chemists and by contributing to the work of technical societies and to the technical press when such contribution does

not conflict with the interests of a client or employer; to announce inventions and scientific advances first in this way rather than through the public press; to ensure that credit for technical work is given to its actual authors;

11. To work for any client or employer under a clear agreement, preferable in writing, as to the ownership of data, plans, improvements, inventions, designs, or other intellectual property developed or discovered while so employed, understanding that in the absence of a written agreement:
 - a. results based on information from the client or employer, not obtainable elsewhere, are the property of the client or employer
 - b. results based on knowledge or information belonging to *The Chemist*, or publicly available, are the property of *The Chemist*, the client or employer being entitled to their use only in the case or project for which *The Chemist* was retained
 - c. all work and results outside of the field for which *The Chemist* was retained or employed, and not using time or facilities belonging to a client or employer, are the property of *The Chemist*;
12. Special data or information provided by a client or employer, or created by *The Chemist* and belonging to the client or employer, must be treated as confidential, used only in general as a part of *The Chemist's* professional experience, and published only after release by the client or employer;
13. To report any infractions of these principles of professional conduct to the authorities responsible for enforcement of applicable laws or regulations, or to the Ethics Committee of The American Institute of Chemists, as appropriate.

Manuscript Style Guide

The Chemist is the official online refereed journal of The American Institute of Chemists (AIC). We accept submissions from all fields of chemistry defined broadly (e.g., scientific, educational, socio-political). *The Chemist* will not consider any paper or part of a paper that has been published or is under consideration for publication anywhere else. The editorial office of *The Chemist* is located at: The American Institute of Chemists, Inc. 315 Chestnut Street Philadelphia, PA 19106-2702, Email: aicoffice@theaic.org.

Categories of Submissions

RESEARCH PAPERS

Research Papers (up to ~5000 words) that are original will only be accepted. Research Papers are peer-reviewed and include an abstract, an introduction, up to 5 figures or tables, sections with brief subheadings and a maximum of approximately 30 references.

REPORTS

Reports (up to ~3000 words) present new research results of broad interest to the chemistry community. Reports are peer-reviewed and include an abstract, an introductory paragraph, up to 3 figures or tables, and a maximum of approximately 15 references.

BRIEF REPORTS

Brief Reports (up to ~1500 words) are short papers that are peer-reviewed and present novel techniques or results of interest to the chemistry community.

REVIEW ARTICLES

Review Articles (up to ~6000 words) describe new or existing areas of interest to the chemistry community. Review Articles are peer-reviewed and include an abstract, an introduction that outlines the main point, brief subheadings for each section and up to 80 references.

LETTERS

Letters (up to ~500 words) discuss material published in *The Chemist* in the last 8 months or issues of general interest to the chemistry community.

BOOK REVIEWS

Book Reviews (up to ~ 500 words) will be accepted.

Manuscript Preparation

RESEARCH PAPERS, REPORTS, BRIEF REPORTS & REVIEW ARTICLES

- **The first page** should contain the title, authors and their respective institutions/affiliations and the corresponding author. The general area of chemistry the article represents should also be indicated, i.e. General Chemistry, Organic Chemistry, Physical Chemistry, Chemical Education, etc.
- **Titles** should be 55 characters or less for Research Papers, Reports, and Brief Reports. Review articles should have a title of up to 80 characters.
- **Abstracts** explain to the reader why the research was conducted and why it is important to the field. The abstract should be 100-150 words and convey the main point of the paper along with an outline of the results and conclusions.
- **Text** should start with a brief introduction highlighting the paper's significance and should be understood to readers of all chemistry disciplines. All symbols, abbreviations, and acronyms should be defined the first time they are used. All tables and figures should be cited in numerical order.
- **Units** must be used appropriately. Internationally accepted units of measurement should be used in conjunction with their numerical values. Abbreviate the units as shown: cal, kcal, μg , mg, g (or gm), %, $^{\circ}\text{C}$, nm, μm (not m), mm, cm, cm^3 , m, in. (or write out inch), h (or hr), min, s (or sec), ml [write out liter(s)], kg. Wherever commonly used units are used their conversion factors must be shown at their first occurrence. Greek symbols are permitted as long as they show clearly in the soft copy.
- **References and notes** should be numbered in the order in which they are cited, starting with the text and then through the table and figure legends. Each reference should have a unique number and any references to unpublished data should be given a number in the text and referred to in the references. References should follow the standards presented in the AIC Reference Style Guidelines below.

REFERENCE STYLE GUIDELINES

References should be cited as numbers within square brackets [] at the appropriate place in the text. The reference numbers should be cited in the correct order throughout the text (including those in tables and figure captions, numbered according to where the table or figure is designated to appear). The references themselves are listed in numerical order at the end of the final printed text along with any Notes. Journal abbreviations should be consistent with those presented in Chemical Abstracts Service Source Index (CASSI) (<http://www.cas.org>) guide available at most academic libraries.

- **Names** and initials of all authors should always be given in the reference and must not be replaced by the phrase *et al.* This does not preclude one from referring to them by the first author, et al in the text.
- **Tables** should be in numerical order as they appear in the text and they should not duplicate the text. Tables should be completely understandable without reading the text. Every table should have a title. Table titles should be placed above the respective tables.

Table 1. Bond Lengths (Å) of 2-aminophenol

- **Figure legends** should be in numerical order as they appear in the text. Legends should be limited to 250 words.

Figure 1. PVC Melt Flow Characterized by Analytical Structural Method

- **Letters and Book Reviews** should be clearly indicated as such when being submitted. They are not peer-reviewed and are published as submitted. Legends should be placed after/under the respective figures.
- **Journals** - The general format for citations should be in the order: **author(s), journal, year, volume, page**. Page number ranges are preferred over single values, but either format is acceptable. Where page numbers are not yet known, articles may be cited by DOI (Digital Object Identifier). For example:

Booth DE, Isenhour TL. *The Chemist*, 2000, 77(6), 7-14.

- **Books** - For example:

Turner GK in *Chemiluminescence: Applications*, ed. Knox Van Dyke, CRC Press, Boca Raton, 1985, vol 1, ch. 3, pp 43-78.

- **Patents** should be indicated in the following form:

McCapra F, Tutt D, Topping RM, UK Patent Number 1 461 877, 1973.

- **Reports and bulletins, etc.** - For example:

Smith AB, Jones CD, *Environmental Impact Report for the US*, final report to the National Science Foundation on Grant AAA-999999, Any University, Philadelphia, PA, 2006.

- **Material presented at meetings** - For example:

Smith AB. Presented at the Pittsburgh Conference, Atlantic City, NJ, March 1983, paper 101.

- **Theses** - For example:

Jones AB, Ph.D. Thesis, Columbia University, 2004.

REFERENCE TO UNPUBLISHED MATERIAL

- For material presented at a meeting, congress or before a Society, etc., but not published, the following form should be used:

Jones AB, presented in part at the 20th American Institute of Chemists National Meeting, Philadelphia, PA, June, 2004.

- For material accepted for publication, but not yet published, the following form should be used:

Smith AB. *Anal. Chem.*, in press

- For material submitted for publication but not yet accepted the following form should be used:

Jones AB, *Anal. Chem.* submitted for publication.

- For personal communications the following should be used:

Smith AB, personal communication.

- If material is to be published but has not yet been submitted the following form should be used:

Smith AB, unpublished work.

Reference to unpublished work should not be made without the permission of those by whom the work was performed.

Manuscript Selection

The submission and review process is completely electronic. Submitted papers are assigned by the Editors, when appropriate, to at least two external reviewers anonymously. Reviewers will have approximately 10 days to submit their comments. In selected situations the review process can be expedited. Selected papers will be edited for clarity, accuracy, or to shorten, if necessary. The Editor-in-Chief will have final say over the acceptance of submissions. Most papers are published in the next issue after acceptance. Proofs will be sent to the corresponding author for review and approval. Authors will be charged for excessive alterations at the discretion of the Editor-in-Chief.

Conditions of Acceptance

When a paper is accepted by *The Chemist* for publication, it is understood that:

- Any reasonable request for materials to verify the conclusions or experiments will be honored.
- Authors retain copyright but agree to allow *The Chemist* to exclusive license to publish the submission in print or online.

- Authors agree to disclose all affiliations, funding sources, and financial or management relationships that could be perceived as potential conflicts of interest or biases.
- The submission will remain a privileged document and will not be released to the public or press before publication.
- The authors certify that all information described in their submission is original research reported for the first time within the submission and that the data and conclusions reported are correct and ethically obtained.
- *The Chemist*, the referees, and the AIC bear no responsibility for accuracy or validity of the submission.

Authorship

By submitting a manuscript, the corresponding author accepts the responsibility that all authors have agreed to be listed and have seen and approved of all aspects of the manuscript including its submission to *The Chemist*.

Submissions

Authors are required to submit their manuscripts, book reviews, and letters electronically. They can be submitted via email at aicoffice@theaic.org with "Submission for consideration in *The Chemist*" in the subject line. All submissions should be in Microsoft® Word format.

Copyright Assignment & Warranty Form for The Chemist

It is the policy of *The Chemist* to require all contributors to transfer the copyright for their contributions (hereafter referred to as the manuscript) to The American Institute of Chemists, Inc. (hereafter referred to as The AIC) the official publisher of *The Chemist*. By signing this agreement, you assign to The AIC to consider publishing your manuscript the exclusive, royalty-free, irrevocable copyright in any medium internationally for the full term of the copyright. This agreement shall permit The AIC to publish, distribute, create derivative works, and otherwise use any materials accepted for publication in *The Chemist* internationally. A copy of the Copyright and Warranty Form for *The Chemist* will be sent to the author(s) whose manuscript is accepted for publication. The AIC will not publish any accepted manuscript in *The Chemist* without its author(s) fully complying with this requirement.

For further information or if you can any questions please contact the Publisher of *The Chemist* at (215) 873-8224 or via email at publications@theaic.org.

Website: <http://www.theaic.org/> Email: aicoffice@theaic.org Phone: 215-873-8224



INVITATION TO AUTHORS

Authors are invited to submit manuscripts for *The Chemist*, the official online refereed journal of The American Institute of Chemists (AIC). We accept submissions from all fields of chemistry defined broadly (e.g., scientific, educational, socio-political). *The Chemist* will not consider any paper or part of a paper that has been published or is under consideration for publication anywhere else.

Research Papers (up to ~5000 words) that are original will only be accepted. Research Papers are peer-reviewed and include an abstract, an introduction, up to 5 figures or tables, sections with brief subheadings and a maximum of approximately 30 references.

Reports (up to ~3000 words) present new research results of broad interest to the chemistry community. Reports are peer-reviewed and include an abstract, an introductory paragraph, up to 3 figures or tables, and a maximum of approximately 15 references.

Brief Reports (up to ~1500 words) are short papers that are peer-reviewed and present novel techniques or results of interest to the chemistry community.

Review Articles (up to ~6000 words) describe new or existing areas of interest to the chemistry community. Review Articles are peer-reviewed and include an abstract, an introduction that outlines the main point, brief subheadings for each section and up to 80 references.

Letters (up to ~500 words) discuss material published in *The Chemist* in the last 8 months or issues of general interest to the chemistry community.

Book Reviews (up to ~ 500 words) will be accepted.

Where to Send Manuscripts?

Please submit your manuscripts by email (aicoffice@theaic.org) to the attention of:

The Editor-in-Chief, *The Chemist*
The American Institute of Chemists, Inc.
315 Chestnut Street
Philadelphia, PA 19106-2702
Email: aicoffice@theaic.org



American Institute of Chemists

www.TheAIC.org

From its earliest days in 1923 to the present, the American Institute of Chemists has fostered the advancement of the chemical profession in the United States.

The Institute has a corresponding dedication "to promote and protect the public welfare; to establish and maintain standards of practice for these professions; and to promote the professional experience through certification as to encourage competent and efficient service."

The AIC engages in a broad range of programs for professional enhancement through the prestigious Fellow membership category, awards program, certification programs, meetings, publications and public relations activities.

Advertising: Send insertion orders and advertising materials to AIC. Visit The AIC Web site for additional information at www.TheAIC.org.

The American Institute of Chemists, Inc.

315 Chestnut Street, Philadelphia, PA 19106-2702.

Phone: (215) 873-8224 | Fax: (215) 629-5224 | E-mail: aicoffice@TheAIC.org